Progress in Fractional Differentiation and Applications
An International Journal

http://dx.doi.org/10.18576/pfda/110107

Mathematical Modeling of Cholera Dynamics and Analysis Using Caputo fractional Operator with Optimal Control

Tulu Leta Tirfe[1], *Legesse Lemecha Obsu*[2], *Eshetu Dadi Gurmu* [2,*], *and Mohamed Hafez*[3]

[1] Department of Mathematic, Bule Hora University, Bule Hora, Ethiopia
[2] Department of Applied Mathematics, Adama Science and Technology Unversity, Adama, Ethiopia
[3] Faculty of Engineering and Quantity Surveying (FEQS), INTI International University, Nilai, Malaysia

Received: 23 Apr. 2024, Revised: 25 May 2024, Accepted: 2 Jun. 2024
Published online: 1 Jan. 2025

Abstract: In this study, we developed a cholera model using the Caputo fractional operator with optimal control strategies to address the dynamic nature of cholera transmission, employing bifurcation analysis. Initially, by applying fixed point theory, we analyzed the existence and uniqueness of the solutions of fractional order derivatives. Furthermore, utilizing the next-generation matrix, we computed the basic reproduction number, crucial for assessing disease dynamics. If this number falls below unity, the equilibrium point remains disease-free, both locally and globally stable, as verified through the Jacobian matrix, Metzler matrix, and Lyapunov function. Otherwise, cholera persistence equilibrium occurs. In addition, we extended the model to include optimal control by integrating three controls: a prevention effort to protect susceptible individuals from contracting the disease and Vibrio cholera, a treatment for those infected with cholera through quarantine, and water sanitation strategies to reduce infectious transmission. These controls were determined using the Pontryagin minimum principle. The model validation was done using numerical experiments. Based on the numerical simulation of fractional order, we observed that the order of derivatives has an impact on controlling disease transmission. The study of this work underscores the benefit of integrating fractional order derivatives with optimal control strategies to mitigate cholera outbreaks effectively. The proposed optimal control framework provides a systematic approach to evaluate the impact of various interventions and inform public health policies. Future research directions include model extensions to incorporate spatial heterogeneity and real-world data integration to further enhance the applicability and robustness of the control strategies.

Keywords: Fractional, cholera, sensitivity,optimal, stability.

1 Introduction

Cholera is a incredibly contagious acute watery dehydrating diarrheal ailment due to Vibrio cholerae and commonly propagated by contaminated water and food [1]. Infectious diseases shows immense diversity, and their outbreaks render millions of people vulnerable to infection, resulting in a significant economic burden on the healthcare system [2].
Nowadays, mathematical modeling plays a vital role in investigating and analyzing the transmission dynamics of diseases, as well as predicting the potential impacts of intervention strategies to manage their distribution. These models help in making informed decisions and establish policies to mitigate the dissemination of diseases, [3,4,5]. In past years, there has been significant study conducted by numerous authors on the complex dynamics of the cholera model. Theoretical analysis of such systems have resulted in a multitude of interesting findings, which have been published in various studies [6,7,8,9], along with the references cited within those publications. These authors have focused on mathematical models that describe the interactions between populations, contaminated water, and poor sanitation. By employing these models, valuable insights into the dynamics of cholera can be obtained, contributing to a better understanding of the disease and the development of effective control strategies.
Tilahun et al. [9] developed a stochastic mathematical model to investigate the behavior of cholera disease, with a specific focus on the direct contact transmission pathway. They extensively studied the qualitative and quantitative

* Corresponding author e-mail: eshetudadi2020@gmail.com

behavior of the model. Adewole and Faniran [11] developed a human host and environment model to examine the complex dynamics of cholera infection. In their model, they considered the fraction of infectious individuals who do not adhere to treatment as part of the overall human population. Their findings suggest that while compliance with treatment is necessary, it alone is not sufficient to eradicate cholera. These studies contribute to the understanding of cholera dynamics by incorporating various factors and transmission pathways into mathematical models. The results emphasize the importance of considering both direct contact transmission and the impact of treatment adherence in devising effective strategies for cholera control.

Fractional operators, which extend the concept of differentiation and integration to non-integer orders, find extensive applications in various fields of knowledge, including physics, biology, finance, and control theory [12,13,14,15]. Their popularity has been on the rise due to their ability to model systems with complex, non-linear, and non-local behavior. One of the main merits of fractional operators is their capability to describe systems with memory effects, which are prevalent in physical and biological systems. Moreover, they can effectively capture the behavior of systems with long-range interactions, making them a valuable tool for modeling complex systems [16,17,18,19]. In [20], a stochastic computational model of cholera infection was proposed in the context of a direct contact transmission pathway applying fractional calculus theory. The study results suggest that policymakers should consider measures such as reducing interactions, improving treatment rates, and encouraging hygiene facilities to eradicate cholera.

Clearly, all of the above-stated works are primarily based fractional derivative and classical integer-order derivatives. However, to some extent, the deterministic model cannot fully account for the natural behavior of the disease [21]. The essential motive is that the community operator of the integer Order calculus does now no longer convey any records approximately the mastering and reminiscence mechanisms of the population that influences disease transmission. Conversely, the non-neighborhood operator of the fractional-order calculus can expound the worldwide traits of sickness transmission process, and the derived results are more general nature. Additionally, they not consider indirect transmission by applying optimal controls and Caputo fractional operators to cholera model with logistic growth for V.cholerae. Thus, to cover the observed gap, we are motivated to propose a cholera model with optimal control and Caputo fractional operators analysis. In this section, the formulated SIQR-B mathematical model of the cholera epidemic model is analyzed to show the impact of optimal control and memory effect on dynamics of cholera infection.

The remainder of this paper is structured as follows: Section 2 presents the formulation of the cholera model in a deterministic and Caputo fractional order framework. In Section 3, we discuss qualitative analysis and sensitivity analysis of the model. Optimal control formulation is detailed in Section 4, followed by numerical simulation results using MATLAB software in Section 5. We present our discussions and conclusions in Section 6. Finally, we present our conclusions in Section 7.

2 Cholera Model Description and Formulation

Based on the condition of their diseases, the model separated all people into four groups. Those are susceptible individuals $S(t)$, are individuals who are vulnerable to the cholera infection over a period of time, infected individuals $I(t)$, are those individuals who have developed the symptom of cholera infection, quarantined individuals $Q(t)$, are individuals who are infectious and compulsory quarantine to reduce the spread of cholera and get treatment based on the patients clinical results, and recovered individuals $R(t)$, are individuals who are recovered from cholera disease by treatment at a time. Moreover, $B(t)$, is the concentration of Vibro cholerae bacterium in an aquatic environment is tracked as an additional compartment.

Moreover, the model assumed that the human population recruited to susceptible compartment at a rate Π and the concentration of the environmental bacteria is described by a logistic growth model with the intrinsic growth rate r and the carrying capacity K. The parameters α_1 and α_2 represents the rate of contribution from an infected individuals and quarantined individuals to the bacteria population in the environment respectively, and μ_B is the bacteria removal rate. Susceptible individuals may acquires cholera infection either directly through human to human transmission at a rate $\beta_2 SI$ or indirectly from environment to human by ingestion of contaminated water and food by Vibrio cholerae bacterium at a rate $\frac{(\beta_1 SB)}{(k+B)}$, where k is the concentration of Vibrios cholera in contaminated water and food that causes 50 percent chance of cholera infection [6], and β_1 ingestion rate. Cholera infected individuals are quarantined to control the transmission of cholera infection and joined the quarantined compartment at a rate θ. Individuals in quarantined compartment recover as a result of cholera treatment at a rate δ. The recovered individuals who lose immunity become susceptible at a rate ω. In all compartments, μ is the natural death rate of individuals, but in the infectious compartment ξ is cholera disease induced death rate. All parameters in the model are non-negative. The schematic diagram of cholera model is shown in Figure (1).

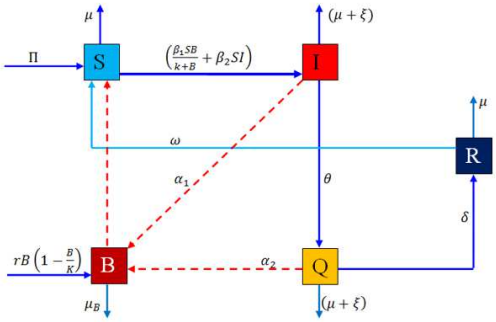

Fig. 1: Schematic Diagram of Cholera Model

Based on the basic assumption with the description and schematic diagram we obtain the following model equations.

$$\begin{cases} \frac{dS(t)}{dt} = \Pi - (\frac{\beta_1 SB}{k+B} + \beta_2 SI) - \mu S + \omega R, \\ \frac{dI(t)}{dt} = (\frac{\beta_1 SB}{k+B} + \beta_2 SI) - (\theta + \alpha_1 + \mu + \xi)I, \\ \frac{dQ(t)}{dt} = \theta I - (\delta + \alpha_2 + \mu + \xi)Q, \\ \frac{dR(t)}{dt} = \delta Q - (\omega + \mu)R, \\ \frac{dB(t)}{dt} = rB(1 - \frac{B}{K}) + \alpha_1 I + \alpha_2 Q - \mu_B B, \end{cases} \tag{1}$$

with initial condition

$$S(0) > 0, I(t) \geq 0, Q(t) \geq 0, R(t) \geq 0, B(t) \geq 0. \tag{2}$$

As a research, fractional derivative modelling capabilities are enhanced by its non-fixed order. The selection of the Caputo operator in this study is motivated by the fact that it permits for the use of local initial conditions to be included in the formulation of the model solution. Besides, the Caputo derivative for a given constant function is zero; thus, it takes the same outcome for integer order derivatives. Upon the memorability nature of the Caputo fractional derivate, model parameters can be estimated well. For this merits, we use the Caputo fractional derivatives to model cholera infection. Taking the above interrelationship and the explanation of the time-dependent kernel defined by the power law correlation function, the new fractional model for the cholera dynamics is as the following system.

$$\begin{cases} {}_0^C D_t^\alpha S(t) = \Pi - (\frac{\beta_1 SB}{k+B} + \beta_2 SI) - \mu S + \omega R, \\ {}_0^C D_t^\alpha I(t) = (\frac{\beta_1 SB}{k+B} + \beta_2 SI) - (\theta + \alpha_1 + \mu + \xi)I, \\ {}_0^C D_t^\alpha Q(t) = \theta I - (\delta + \alpha_2 + \mu + \xi)Q, \\ {}_0^C D_t^\alpha R(t) = \delta Q - (\omega + \mu)R, \\ {}_0^C D_t^\alpha B(t) = rB(1 - \frac{B}{K}) + \alpha_1 I + \alpha_2 Q - \mu_B B, \end{cases} \tag{3}$$

with initial condition

$$S(0) > 0, I(t) \geq 0, Q(t) \geq 0, R(t) \geq 0, B(t) \geq 0. \tag{4}$$

where all the parameters are assumed to be non-negative, and ${}_0^C D_t^\alpha$ denotes the Caputo fractional derivative (CFD) of order $\alpha \in (0,1]$ for function $f(t)$ such that [8].

2.1 Preliminaries

In this section, we review several key definitions, lemmas, and concepts that are necessary to understand our suggested model.

Definition 1.*([42,43]). Given a function $u : \Re^+ \longrightarrow \Re$, and $\alpha \in (n-1, n), n \in N$. The left Caputo fractional derivative of order α of the function u is defined as,*

$$ {}_0^C D_t^\alpha(u(t)) = \frac{1}{\Gamma(n-\alpha)} \int_0^t u^n(k)(t-k)^{n-\alpha-1)} dk, $$

and the Mittag-Leffler function $E_\alpha(z)$ *with* $\mathbf{C}$ *the set of the complex number is given by,*

$$ E_\alpha(z) = \sum_{\beta=0}^{\infty} \frac{z^\beta}{\Gamma(1+\alpha\beta)}, \alpha, z \in \mathbf{C}, \Re(\alpha) > 0. $$

Definition 2.*([42,43]). The corresponding Riemann-Liouville fractional integral associated with the power-law kernel is defined as,*

$$ {}_0^C I_t^\alpha(u(t)) = \frac{1}{\Gamma(\alpha)} \int_0^t (t-k)^{\alpha-1)} u(k) dk, t > 0. $$

Definition 3.*The Laplace transform of the Caputo fractional derivative is,*

$$ \left\{ {}_0^C D_t^\alpha u(t); s \right\} = s^\alpha F(s) - \sum_{k=0}^{n-1} s^{\alpha-k-1} f^(k)(0), $$

where $n-1 < \alpha \leq n$.

Lemma 1.*([45,46]). Assuming there is a function* $u(t) \in C[0,\eta]$ *of order* $\alpha \in (0,1)$*, the solution of fractional differential equation,*

$$ \begin{cases} {}_0^C D_t^\alpha(u(t)) = Y(t,u(t)), t \in [0,\eta], \\ u(0) = u_0, \end{cases} $$

is given by

$$ u(t) - u(0) = \frac{1}{\Gamma(\alpha)} \int_0^t Y(k,u(k))(t-k)^{\alpha-1} dk. $$

3 Basic Properties of Cholera Model

3.1 Existence and Uniqueness of the Solutions

This part shows that the system has a unique solution. First, we construct the system (3) as follows;

$$ \begin{cases} {}_0^C D_t^\alpha S(t) = F_1(t,S(t)), \\ {}_0^C D_t^\alpha I(t) = F_2(t,I(t)), \\ {}_0^C D_t^\alpha Q(t) = F_3(t,Q(t)), \\ {}_0^C D_t^\alpha R(t) = F_4(t,R(t)), \\ {}_0^C D_t^\alpha B(t) = F_5(t,B(t)), \\ F_1(t,S(t)) = \Pi - (\frac{\beta_1 SB}{k+B} + \beta_2 SI) - \mu S + \omega R, \\ F_2(t,I(t)) = (\frac{\beta_1 SB}{k+B} + \beta_2 SI) - (\theta + \alpha_1 + \mu + \xi) I, \\ F_3(t,Q(t)) = \theta I - (\delta + \alpha_2 + \mu + \xi) Q, \\ F_4(t,R(t)) = \delta Q - (\omega + \mu) R, \\ F_5(t,B(t)) = rB(1 - \frac{B}{K}) + \alpha_1 I + \alpha_2 Q - \mu_B B. \end{cases} $$

Taking the both sides of the previous equations as an integral form, we get

$$ \begin{cases} S(t) - S(0) = \frac{1}{\Gamma(\alpha)} \int_0^t (t-k)^{\alpha-1} F_1(k,S) dk, \\ I(t) - I(0) = \frac{1}{\Gamma(\alpha)} \int_0^t (t-k)^{\alpha-1} F_2(k,I) dk, \\ Q(t) - Q(0) = \frac{1}{\Gamma(\alpha)} \int_0^t (t-k)^{\alpha-1} F_3(k,Q) dk, \\ R(t) - R(0) = \frac{1}{\Gamma(\alpha)} \int_0^t (t-k)^{\alpha-1} F_4(k,R) dk, \\ B(t) - B(0) = \frac{1}{\Gamma(\alpha)} \int_0^t (t-k)^{\alpha-1} F_5(k,S) dk, \end{cases} \tag{5} $$

we show that the kernel $F_i, fori = 1,2,3,4,5$ follows the condition of Lipschitz and contraction.

Theorem 1.*If the following inequality holds* $0 \leq r_i < 1$*, then the function* F_i *for* $i = 1,2,3,4,5$ *fulfill with the condition of Lipschitz and contraction mapping as well.*

*Proof.*We have for S and S_1

$$\begin{aligned} \| F_1(t,S) - F_1(t,S_1) \| &= \| (\tfrac{\beta_1 B}{k+B} + \beta_2 I)(S_1 - S) + \mu(S_1 - S) \| \\ &\leq [\| (\tfrac{\beta_1 B}{k+B} + \beta_2 I) \| + \| \mu \|] \| (S_1 - S) \| \\ &\leq [(\tfrac{\| \beta_1 \| \| B \|}{\| k \| + \| B \|} + \| \beta_2 \| \| I \|) + \| \mu \|] \| (S_1 - S) \| \\ &\leq [(\tfrac{\beta_1 \| B \|}{k + \| B \|} + \beta_2 \| I \|) + \mu] \| (S_1 - S) \| \\ &\leq [(\tfrac{\beta_1 z_5}{k+z_5} + \beta_2 z_2) + \mu] \| (S_1 - S) \| . \end{aligned}$$

Where there are positive constants z_1, z_2, z_3, z_4, z_5 such as

$$\begin{cases} \| S(t) \| \leq z_1, \| I(t) \| \leq z_2, \\ \| Q(t) \| \leq z_3, \| R(t) \| \leq z_4, \| B(t) \| \leq z_5, \end{cases}$$

and $r_1 = ((\frac{\beta_1 z_5}{k+z_5} + \beta_2 z_2) + \mu)$ are non-negative bounded functions.
Hence

$$\| F_1(t,S) - F_1(t,S_1) \| \leq r_1 \| S(t) - S_1(t) \| . \tag{6}$$

Similarly, we can prove that F_i , for $i = 2,3,4,5$ fulfill the Lipschitz condition as following:

$$\begin{cases} \| F_2(t,I) - F_2(t,I_1) \| \leq r_2 \| I(t) - I_1(t) \|, \\ \| F_3(t,Q) - F_3(t,Q_1) \| \leq r_3 \| Q(t) - Q_1(t) \|, \\ \| F_4(t,R) - F_4(t,R_1) \| \leq r_4 \| R(t) - R_1(t) \|, \\ \| F_5(t,B) - F_5(t,B_1) \| \leq r_5 \| B(t) - B_1(t) \| . \end{cases}$$

Therefore, F_i satisfies the Lipschitz condition. Furthermore, under the condition $0 \leq r_i \ll 1$, the functions are contractions. Depending on the system (3), consider the following recursive forms:

$$\begin{cases} S_n(t) = \frac{1}{\Gamma(\alpha)} \int_0^t (t-k)^{\alpha-1} F_1(k, S_{n-1}) dk, \\ I_n(t) = \frac{1}{\Gamma(\alpha)} \int_0^t (t-k)^{\alpha-1} F_2(k, I_{n-1}) dk, \\ Q_n(t) = \frac{1}{\Gamma(\alpha)} \int_0^t (t-k)^{\alpha-1} F_3(k, Q_{n-1}) dk, \\ R_n(t) = \frac{1}{\Gamma(\alpha)} \int_0^t (t-k)^{\alpha-1} F_4(k, R_{n-1}) dk, \\ B_n(t) = \frac{1}{\Gamma(\alpha)} \int_0^t (t-k)^{\alpha-1} F_5(k, B_{n-1}) dk. \end{cases}$$

The difference between two terms can be expressed as follows:

$$\begin{cases} \Phi_{1n}(t) = S_n(t) - S_{n-1}(t) = \frac{1}{\Gamma(\alpha)} \int_0^t (t-k)^{\alpha-1} (F_1(k, S_{n-1}) - F_1(k, S_{n-2})) dk, \\ \Phi_{2n}(t) = I_n(t) - I_{n-1}(t) = \frac{1}{\Gamma(\alpha)} \int_0^t (t-k)^{\alpha-1} (F_2(k, I_{n-1}) - F_2(k, I_{n-2})) dk, \\ \Phi_{3n}(t) = Q_n(t) - Q_{n-1}(t) = \frac{1}{\Gamma(\alpha)} \int_0^t (t-k)^{\alpha-1} (F_3(k, Q_{n-1}) - F_3(k, Q_{n-2})) dk, \\ \Phi_{4n}(t) = R_n(t) - R_{n-1}(t) = \frac{1}{\Gamma(\alpha)} \int_0^t (t-k)^{\alpha-1} (F_4(k, R_{n-1}) - F_4(k, R_{n-2})) dk, \\ \Phi_{5n}(t) = B_n(t) - B_{n-1}(t) = \frac{1}{\Gamma(\alpha)} \int_0^t (t-k)^{\alpha-1} (F_5(k, B_{n-1}) - F_5(k, B_{n-2})) dk, \end{cases}$$

using the initial condition $S(t) = S(0), I(t) = I(0), Q(t) = Q(0), R(t) = R(0), B(t) = B(0)$. We continue the first equation of the preceding method with the norm and through Lipschitz condition (13), we get;

$$\begin{aligned} \| \Phi_{1n}(t) \| = \| S_n(t) - S_{n-1}(t) \| &= \| \tfrac{1}{\Gamma(\alpha)} \int_0^t (t-k)^{\alpha-1} (F_1(k, S_{n-1}) - F_1(k, S_{n-2})) dk \|, \\ &\leq \tfrac{1}{\Gamma(\alpha)} \int_0^t \| (t-k)^{\alpha-1} (F_1(k, S_{n-1}) - F_1(k, S_{n-2}) \|) dk, \\ \| \Phi_{1n}(t) \| &\leq \tfrac{r_1}{\Gamma(\alpha)} \int_0^t \| \Phi_1(n-1)(k) \| dk, \end{aligned} \tag{7}$$

likewise, we get

$$\begin{array}{l} \| \Phi_{2n}(t) \| \leq \frac{r_2}{\Gamma(\alpha)} \int_0^t \| \Phi_2(n-1)(k) \| dk, \\ \| \Phi_{2n}(t) \| \leq \frac{r_2}{\Gamma(\alpha)} \int_0^t \| \Phi_2(n-1)(k) \| dk, \\ \| \Phi_{3n}(t) \| \leq \frac{r_3}{\Gamma(\alpha)} \int_0^t \| \Phi_3(n-1)(k) \| dk, \\ \| \Phi_{4n}(t) \| \leq \frac{r_4}{\Gamma(\alpha)} \int_0^t \| \Phi_4(n-1)(k) \| dk, \\ \| \Phi_{5n}(t) \| \leq \frac{r_5}{\Gamma(\alpha)} \int_0^t \| \Phi_5(n-1)(k) \| dk. \end{array} \tag{8}$$

Then we can write that;

$$\begin{cases} S_n(t) = \sum_{i=1}^n \Phi_{1i}(t), I_n(t) = \sum_{i=1}^n \Phi_{2i}(t), \\ Q_n(t) = \sum_{i=1}^n \Phi_{3i}(t), R_n(t) = \sum_{i=1}^n \Phi_{4i}(t), B_n(t) = \sum_{i=1}^n \Phi_{5i}(t). \end{cases}$$

In the following theorem, we prove the existence of a solution.

Theorem 2.*If there exists $t_1 > 1$ such that $\frac{r_i}{\Gamma(\alpha)} t_1 \leq 1$, for $i = 1,2,3,4,5$ then, there exist at least one solution of system given by the fractional cholera SIQR-B.*

*Proof.*Suppose their exist t such that $\frac{r_i}{\Gamma(\alpha)} t_1 \leq 1$.
From the recursive scheme and from (7) as well as (8), we have obtained that $\| \Phi_{1n}(t) \| \leq \frac{r_1}{\Gamma(\alpha)} \int_0^t \| \Phi_1(n-1)(k) \| dk$.
Replacing n by n - 1 in the above inequality

$$\begin{array}{c} \| \Phi_{n-1}(t) \| \leq \frac{r_1}{\Gamma(\alpha)} \int_0^t \| \Phi_1(n-2)(k) \| dk, \\ \leq (\frac{r_1}{\Gamma(\alpha)})^2 \int_0^t \| \Phi_1(n-2)(k) \| dk. \end{array}$$

Again replacing n by n - 2 in the given inequality

$$\begin{array}{c} \| \Phi_{n-2}(t) \| \leq \frac{r_1}{\Gamma(\alpha)} \int_0^t \| \Phi_1(n-3)(k) \| dk, \\ \leq (\frac{r_1}{\Gamma(\alpha)})^3 \int_0^t \| \Phi_1(n-3)(k) \| dk. \end{array}$$

If we keep substituting in this way and use the initial condition, we obtain

$$\| \Phi_{1n}(t) \| \leq \| S_n(0) \| [\frac{r_1}{\Gamma(\alpha)} t]^n.$$

Similarly, we get

$$\begin{array}{l} \| \Phi_{2n}(t) \| \leq \| I_n(0) \| [\frac{r_2}{\Gamma(\alpha)}]^n, \\ \| \Phi_{3n}(t) \| \leq \| Q_n(0) \| [\frac{r_3}{\Gamma(\alpha)}]^n, \\ \| \Phi_{4n}(t) \| \leq \| R_n(0) \| [\frac{r_4}{\Gamma(\alpha)}]^n, \\ \| \Phi_{5n}(t) \| \leq \| B_n(0) \| [\frac{r_5}{\Gamma(\alpha)}]^n. \end{array}$$

This system has a solution, so it is also continuous. We will show that $\Phi_{1n}(t), \Phi_{2n}(t), \Phi_{3n}(t), 4n(t), \Phi_{5n}(t)$ converge to system of solution (3).
Consider $D_{1n(t)}, D_{2n(t)}, D_{3n(t)}, D_{4n(t)}, D_{5n(t)}$, as fixed point iteration method, so that

$$\begin{cases} S(t) - S(0) = S_n(t) - D_{1n}(t), \\ I(t) - I(0) = I_n(t) - D_{1n}(t), \\ Q(t) - Q(0) = Q_n(t) - D_{1n}(t), \\ R(t) - R(0) = R_n(t) - D_{1n}(t), \\ B(t) - S(0) = B_n(t) - D_{1n}(t). \end{cases} \tag{9}$$

Using the triangular inequality with the condition of Lipschitz F_1, we are getting:

$$\begin{array}{c} \| D_{1n}(t) \| = \| \frac{1}{\Gamma(\alpha)} \int_0^t (F_1(k,S_n) - F_1(k,S_{n-1}))dk \|, \\ \leq \frac{1}{\Gamma(\alpha)} \int_0^t (F_1(k,S_n) - F_1(k,S_{n-1}) \|))dk, \\ \leq \frac{r_1}{\Gamma(\alpha)} r_1 \| S_n - Sn - 1 \| t. \end{array}$$

By applying the above process recursively, we obtain

$$\| D_{1n}(t) \| = \leq [\tfrac{r_1}{\Gamma(\alpha)} r_1]^{n+1} k,$$

here K is the Lipschitz constant.
As a result, the sequence is valid and follows the described conditions as

$$\| D_{2n}(t) \| \longrightarrow 0, \| D_{3n}(t) \| \longrightarrow 0, \| D_{4n}(t) \| \longrightarrow 0, \| D_{5n}(t) \| \longrightarrow 0,$$

as $n \longrightarrow \infty$.

$$\begin{cases} \| S_{n+r}(t) - S_n(t) \| \leq \sum_{i=n+1}^{n+r} Y_1^i = \frac{Y_1^{n+1} - Y_1^{n+r+1}}{1-Y_1}, \\ \| I_{n+r}(t) - I_n(t) \| \leq \sum_{i=n+1}^{n+r} Y_2^i = \frac{Y_2^{n+1} - Y_2^{n+r+1}}{1-Y_1}, \\ \| Q_{n+r}(t) - Q_n(t) \| \leq \sum_{i=n+1}^{n+r} Y_3^i = \frac{Y_3^{n+1} - Y_3^{n+r+1}}{1-Y_3}, \\ \| R_{n+r}(t) - R_n(t) \| \leq \sum_{i=n+1}^{n+r} Y_4^i = \frac{Y_4^{n+1} - Y_4^{n+r+1}}{1-Y_4}, \\ \| B_{n+r}(t) - B_n(t) \| \leq \sum_{i=n+1}^{n+r} Y_5^i = \frac{Y_5^{n+1} - Y_5^{n+r+1}}{1-Y_5}. \end{cases}$$

By hypothesis $\frac{r_i}{\Gamma(\alpha)} t_1 \leq 1$, S, I, Q, R, B are Cauchy sequences. For this reason, it can be deduce that they are uniformly convergent. Hence, the limit of the sequences is the unique solution of the fractional system (3).

Theorem 3.*If the condition* $(1 - \frac{r_i}{\Gamma(\alpha)})t > 0$, *for* $i = 1,2,3,4,5$ *holds then the SIQRB model of Cholera is unique solution.*

*Proof.*We assume that another solution is possible for the system to highlight the uniqueness of the solution, such a $S_1(t), I_1(t), Q_1(t), R_1(t)$ and $B_1(t)$ then we have

$$S(t) - S_1(t) = \frac{1}{\Gamma(\alpha)} \int_0^t (F_1(t,S) - F_1(t,S_1)) dk.$$

Now, we take the norm of above equation

$$\| S(t) - S_1(t) \| = \| \tfrac{1}{\Gamma(\alpha)} \int_0^t (F_1(t,S) - F_1(t,S_1)) \| dk, \leq \tfrac{1}{\Gamma(\alpha)} \int_0^t \| (F_1(t,S) - F_1(t,S_1)) \| dk.$$

From the Lipschitz condition (7) it follows that,

$$\| S(t) - S_1(t) \| \leq \tfrac{1}{\Gamma(\alpha)} r_1 t \| (S(t) - S_1(t)) \|,$$

consequently,

$$\| S(t) - S_1(t) \| \tfrac{1}{\Gamma(\alpha)} r_1 t \| (S(t) - S_1(t)) \| \leq 0,$$

$$\| S(t) - S_1(t) \| [1 - \frac{1}{\Gamma(\alpha)} r_1 t] \leq 0. \tag{10}$$

By the hypothesis $(1 - \frac{r_i}{\Gamma(\alpha)})t > 0$ the previous (7) become the form,

$$\| S(t) - S_1(t) \| = 0.$$

This means that $S(t) = S_1(t)$. Apply similar technique to all solution for $i = 2,3,4,5$ we get
$\| I(t) - I_1(t) \| = 0, \| Q(t) - Q_1(t) \| = 0, \| Q(t) - Q_1(t) \| = 0, \| Q(t) - Q_1(t) \| = 0$. Hence, the theorem is proved. Therefore based on analysis and discussion described above, the solutions of the system (3) remain positive and bounded. Hence, system (3) is both mathematically and epidemiologically well-posed.

3.2 Invariant region

In the following analyses, we shall demonstrate that the model performs well-posed in both epidemiologically and mathematically.

Theorem 4.*The epidemiologically feasible region of model (3) is given by*

$$\Omega = \left\{ (S,I,Q,R,B) \in R_+^5 : 0 \leq N(t) \leq \frac{\Pi}{\mu}, B(t) \leq \frac{(\alpha_1+\alpha_2)}{\mu\mu_B r}\Pi K \right\}. \tag{11}$$

*Proof.*The boundedness of the solutions are performed in two parts: the human population and bacterial population. For the human population, the first four equations of system (3) are summed to give

$${}_0^C D_t^\alpha N(t) = \Pi - \mu N(t) - I\alpha_1 - \xi I - \alpha_2 Q - \xi Q \leq \Pi - \mu N(t). \tag{12}$$

Applying the Laplace transform of the above inequality, we have

$$\lambda^\alpha \ell[N(t)] - \lambda^{\alpha-1} N(0) \leq \frac{\Pi}{\lambda} - \mu\ell[N(t)], \tag{13}$$

that can be written as

$$\ell[N(t)] \leq \frac{\lambda^{-1}}{\lambda^\alpha + \mu}\Pi + \frac{\lambda^{\alpha-1}}{\lambda^\alpha+\mu} N(0), \tag{14}$$

applying the inverse of the Laplace transform on inequality (6) gives

$$N(t) \leq \Pi t^\alpha E_{\alpha,\alpha+1}(-\mu t^\alpha) + E_{\alpha,1}(-\mu t^\alpha)N(0) = (-\frac{\Pi}{\mu} + N(0))E_{\alpha,1}(-\mu t^\alpha) + \frac{\Pi}{\mu}, \tag{15}$$

where

$$E_{a,b}(z) = \sum_{k=0}^{\infty} \frac{z^k}{\Gamma(ak+b)}$$

is Mittag-Leffler function with parameters a and b. It is clear that $N(0) \leq \frac{\Pi}{\mu}$ when $t = 0$. Then, $N(t) \leq \frac{\Pi}{\mu}$ can be derived from $E_{\alpha,1}(-\mu t^(\alpha)) \geq 0$.
Next, for the bacterial population, it follows that

$${}_0^C D_t^\alpha B(t) \leq rB(1 - \frac{B}{K}) + \alpha_1 I + \alpha_2 Q - \mu_B B, \tag{16}$$

thus, one has

$$B(t) \leq \frac{(\alpha_1+\alpha_2)}{\mu\mu_B r}\Pi K.$$

As such, the feasible region for system (3) is given by

$$\Omega = \left\{ (S,I,Q,R,B) \in R_+^5 : 0 \leq N(t) \leq \frac{\Pi}{\mu}, B(t) \leq \frac{(\alpha_1+\alpha_2)}{\mu\mu_B r}\Pi K \right\}. \tag{17}$$

3.3 Positivity of Solutions

Theorem 5.*For the given initial conditions (4), the solutions of system (3) are positive and bounded for all* $t \geq 0$.

*Proof.*One of the important characteristics of epidemiological models is that their solutions are both positive and bounded. In order to ensure this, we establish that all of the state variables are non-negative for any time $m > 0$, which implies that a trajectory starting with a positive initial condition will stay positive for all $m > 0$. Thus, system (3) gives

$$\begin{cases} {}_0^C D_t^\alpha S(t)|S=0 = \Pi + \omega R \geq 0, \\ {}_0^C D_t^\alpha I(t)|I=0 = \frac{\beta_1 SB}{k+B} \geq 0, \\ {}_0^C D_t^\alpha Q(t)|Q=0 = \theta I \geq 0, \\ {}_0^C D_t^\alpha R(t)|R=0 = \delta Q \geq 0, \\ {}_0^C D_t^\alpha B(t)|B=0 = \alpha_1 I + \alpha_2 Q \geq 0. \end{cases} \tag{18}$$

Based on analysis and discussion described above, the solutions of the system (3) remain positive and bounded.

3.4 Cholera Disease-free equilibrium point

A disease-free equilibrium $E_0 = (S_0, I_0, Q_0, R_0, B_0)$ of cholera model is a point where cholera infection is not in the population. Hence, setting
${}_0^C D_t^\alpha S(t) = 0, {}_0^C D_t^\alpha I(t) = 0, {}_0^C D_t^\alpha Q(t) = 0, {}_0^C D_t^\alpha R(t) = 0, {}_0^C D_t^\alpha B(t) = 0, I = 0, B = 0$ in the cholera model (3), then computed cholera-free equilibrium is given by

$$\begin{cases} {}_0^C D_t^\alpha S(t) = 0, \\ {}_0^C D_t^\alpha I(t) = 0, \\ {}_0^C D_t^\alpha Q(t) = 0, \\ {}_0^C D_t^\alpha R(t) = 0, \\ {}_0^C D_t^\alpha B(t) = 0. \end{cases} \tag{19}$$

Which means

$$\begin{cases} \Pi - (\frac{\beta_1 SB}{k+B} + \beta_2 SI) - \mu S + \omega R = 0, \\ (\frac{\beta_1 SB}{k+B} + \beta_2 SI) - (\theta + \alpha_1 + \mu + \xi) I = 0, \\ \theta I - (\delta + \alpha_2 + \mu + \xi) Q = 0, \\ \delta Q - (\omega + \mu) R = 0, \\ rB(1 - \frac{B}{K}) + \alpha_1 I + \alpha_2 Q - \mu_B B = 0. \end{cases} \tag{20}$$

Then the system of equations (20) is simplified, which gives
$\Pi - (\frac{\beta_1 SB}{k+B} + \beta_2 SI) - \mu S + \omega R = 0,$
by solving above equation we get
$S_0 = \frac{\Pi}{\mu}$.
Therefore, our disease-free equilibrium point is $E_0 = (\frac{\Pi}{\mu}, 0, 0, 0, 0)$.

3.5 Endemic Equilibrium

The endemic equilibrium point $E^* = (S^*, I^*, Q^*, R^*, B^*)$ of cholera model is the point where the infection persists in the population or where rate of change of fractional derivatives vanish and it is obtained by solving the following equations:

$$\begin{cases} \Pi - (\frac{\beta_1 SB}{k+B} + \beta_2 SI) - \mu S + \omega R = 0, \\ (\frac{\beta_1 SB}{k+B} + \beta_2 SI) - (\theta + \alpha_1 + \mu + \xi)I = 0, \\ \theta I - (\delta + \alpha_2 + \mu + \xi)Q = 0, \\ \delta Q - (\omega + \mu)R = 0, \\ rB(1 - \frac{B}{K}) + \alpha_1 I + \alpha_2 Q - \mu_B B = 0. \end{cases} \tag{21}$$

Hence, the solution of preceding equation is given by

$$E^* = (S^*, I^*, Q^*, R^*, B^*). \tag{22}$$

Where

$$\begin{cases} Q^* = \frac{(\omega+\mu)R^*}{\delta}, \\ I^* = \frac{(\delta+\alpha_2+\mu+\xi)(\omega+\mu)R^*}{\theta\delta}, \\ B^* = (r-\mu_B) + \sqrt{(\mu_B - r)^2 + \frac{4r}{K}(\frac{\alpha_1 b(\omega+\mu)R^*}{\theta\delta} + \frac{\alpha_2(\omega+\mu)R^*}{\delta})}, \\ S^* = \frac{(\theta+\alpha_1+\mu+\xi)I^*}{\frac{\beta_1 B^*}{k+B^*} + \beta_2 I^*}, \\ R^* = \frac{(\frac{\beta_1 S^* B^*}{k+B^*} + \beta_2 S^* I^*) + \mu S^* - \Pi}{\omega}, \end{cases} \tag{23}$$

where, $b = \delta + \alpha_2 + \mu + \xi$.

3.6 Basic Reproduction Number

Here, the threshold parameter that governs the spread of disease known as the basic reproduction number is obtained. It is nothing but the spectral radius of the next-generation matrix. For the purpose, the system of model (3) is rearranged starting with those representing newly infective classes.

$$\begin{array}{rl} {}_0^C D_t^\alpha I(t) & = (\frac{\beta_1 SB}{k+B} + \beta_2 SI) - (\theta + \alpha_1 + \mu + \xi)I, \\ {}_0^C D_t^\alpha Q(t) & = \theta I - (\delta + \alpha_2 + \mu + \xi)Q, \\ {}_0^C D_t^\alpha B(t) & = rB(1 - \frac{B}{K}) + \alpha_1 I + \alpha_2 Q - \mu_B B. \end{array} \tag{24}$$

Let $Z = [I, Q, B]^T$ denote a vector of infectious variables,

$${}_0^C D_t^\alpha Z = F(Z) - V(Z) = \begin{bmatrix} \frac{\beta_1 SB}{k+B} + \beta_2 SI \\ 0 \end{bmatrix} - \begin{bmatrix} (\theta + \alpha_1 + \mu + \xi)I \\ -\theta I + (\delta + \alpha_2 + \mu + \xi)Q \\ -rB(1 - \frac{B}{K}) - \alpha_1 I - \alpha_2 Q + \mu_B B \end{bmatrix},$$

with the next-generation matrices,

$$F = \frac{\partial F(Z)}{\partial Z}|_{E_0} = \begin{bmatrix} \beta_2 S_0 & 0 & \frac{\beta_1 S_0}{K} \\ 0 & 0 & 0 \\ 0 & 0 & 0 \end{bmatrix}, V = \frac{\partial V(Z)}{\partial Z}|_{E_0} = \begin{bmatrix} \theta + \alpha_1 + \mu + \xi & 0 & 0 \\ -\theta & \delta + \alpha_2 + \mu + \xi & 0 \\ -\alpha_1 & -r + \mu_B & -\alpha_2 \end{bmatrix},$$

which leads to,

$$FV^{-1} = \begin{bmatrix} \beta_2 S_0(\delta + \alpha_2 + \mu + \xi) + \frac{\beta_1 S_0(-\theta(-r+\mu_B) + \alpha_1(\delta+\alpha_2+\mu+\xi))}{K(\theta+\alpha_1+\mu+\xi)(-\alpha_2\delta - \alpha_2^2 - \mu\alpha_2 - \xi\alpha_2)} & \frac{\beta_1 S_0(-r+\mu_B)}{K(\alpha_2\delta + \alpha_2^2 + \mu\alpha_2 + \xi\alpha_2)} & \frac{-\beta_1 S_0 \alpha_2}{K} \\ 0 & 0 & 0 \\ 0 & 0 & 0 \end{bmatrix}, \text{then, } R_0$$

Here, by the next generation matrix principle, the largest eigenvalue is the basic reproduction number. Therefore, our basic reproduction number is

$$R_0 = \frac{\beta_1 \Pi\theta(-r+\mu_B) + \beta_2 \Pi(\delta + \alpha_2 + \mu + \xi)^2 \alpha_2 K(\theta + \alpha_1 + \mu + \xi) - \beta_1 \Pi\alpha_1(\delta + \alpha_2 + \mu + \xi)}{\alpha_2 \mu K(\theta + \alpha_1 + \mu + \xi)(\delta + \alpha_2 + \mu + \xi)} \tag{25}$$

or

$$R_0 = \frac{\beta_1 \Pi\theta(-r+\mu_B) + \beta_2 \Pi m^2 \alpha_2 Kn - \beta_1 \Pi\alpha_1 m}{\alpha_2 \mu Knm},$$

where
$m = \delta + \alpha_2 + \mu + \xi, n = \theta + \alpha_1 + \mu + \xi$.

3.7 Local Stability of Disease-Free Equilibrium

Theorem 6.*Disease-free equilibrium E_0 of system of equations given in (1) is locally asymptotically stable if $R_0 < 1$ and unstable if $R_0 > 1$.*

*Proof.*To show that the DFE point of our model system 3 is locally asymptotically stable, we need to show that all the eigenvalues of Jacobian matrix J of system of Equation (3) evaluated at DFE point satisfies the condition $|arg(\lambda_i)| > \alpha \frac{\pi}{2}$. Let us find the Jacobian matrix J of model system of Equation (3) at DFE point. Jacobian matrix J of (3) evaluated at DFE point is given by

$$\begin{cases} {}_0^C D_t^\alpha S(t) = \Pi - (\frac{\beta_1 SB}{k+B} + \beta_2 SI) - \mu S + \omega R = f_1, \\ {}_0^C D_t^\alpha I(t) = (\frac{\beta_1 SB}{k+B} + \beta_2 SI) - (\theta + \alpha_1 + \mu + \xi) I = f_2, \\ {}_0^C D_t^\alpha Q(t) = \theta I - (\delta + \alpha_2 + \mu + \xi) Q = f_3, \\ {}_0^C D_t^\alpha R(t) = \delta Q - (\omega + \mu) R = f_4, \\ {}_0^C D_t^\alpha B(t) = rB(1 - \frac{B}{K}) + \alpha_1 I + \alpha_2 Q - \mu_B B = f_5. \end{cases}$$

Then the Jacobian matrix is given by equation(26).

$$J = \begin{bmatrix} -[\frac{\beta_1 B}{k+B} + \beta_2 I] - \mu & -\beta_2 S & 0 & \omega & \frac{-\beta_1 S(k+B) + \beta_1 SB}{(K+B)^2} \\ \frac{\beta_1 B}{k+B} + \beta_2 I & \beta_2 S - (\theta + \alpha_1 + \mu + \xi) & 0 & 0 & \frac{\beta_1 S(K+B) - \beta_1 SB}{(k+B)^2} \\ 0 & \theta & -(\delta + \alpha_2 + \mu + \xi) & 0 & 0 \\ 0 & 0 & \delta & -(\omega + \mu) & 0 \\ 0 & \alpha_1 & \alpha_2 & 0 & r - \frac{2Br}{K} - \mu_B \end{bmatrix} \tag{26}$$

Then the Jacobian matrix evaluated at E_0 becomes

$$J(E_0) = \begin{bmatrix} -\mu & -\frac{\beta_2 \Pi}{\mu} & 0 & \omega & \frac{-\beta_1 \Pi}{\mu k} \\ 0 & \frac{\beta_2 \Pi}{\mu} - (\theta + \alpha_1 + \mu + \xi) & 0 & 0 & \frac{\beta_1 \Pi}{\mu k} \\ 0 & \theta & -(\delta + \alpha_2 + \mu + \xi) & 0 & 0 \\ 0 & 0 & \delta & -(\omega + \mu) & 0 \\ 0 & \alpha_1 & \alpha_2 & 0 & r - \mu_B \end{bmatrix} \tag{27}$$

From equation(27) the eigenvalues are evaluated as follows:

$$J(E_0) = \begin{vmatrix} -\mu - \lambda & -\frac{\beta_2 \Pi}{\mu} & 0 & \omega & \frac{-\beta_1 \Pi}{\mu k} \\ 0 & \frac{\beta_2 \Pi}{\mu} - (\theta + \alpha_1 + \mu + \xi) - \lambda & 0 & 0 & \frac{\beta_1 \Pi}{\mu k} \\ 0 & \theta & -(\delta + \alpha_2 + \mu + \xi) - \lambda & 0 & 0 \\ 0 & 0 & \delta & -(\omega + \mu) - \lambda & 0 \\ 0 & \alpha_1 & \alpha_2 & 0 & -(\mu_B - r) - \lambda \end{vmatrix} \tag{28}$$

The Characteristic Polynomial of equation (28)becomes

$$(-\mu - \lambda)(\frac{\beta_2 \Pi}{\mu} - (\theta + \alpha_1 + \mu + \xi) - \lambda)(-(\delta + \alpha_2 + \mu + \xi) - \lambda)(-(\omega + \mu) - \lambda)(-(\mu_B - r) - \lambda) = 0. \tag{29}$$

By factorizing the Characteristic Polynomial of equation,eigenvalues are as follows:
$\lambda_1 = -\mu, \lambda_2 = -((\theta + \alpha_1 + \mu + \xi) - \frac{\beta_2 \Pi}{\mu}), \lambda_3 = -(\delta + \alpha_2 + \mu + \xi), \lambda_4 = -(\omega + \mu), \lambda_5 = -(\mu_B - r)$
Since
$\lambda_1 < 0, \lambda_2 < 0, \lambda_3 < 0, \lambda_4 < 0, \lambda_5 < 0$ for $\mu_B < r$, know the sign of all eigenvalues are negative.
Therefore,our disease-free equilibrium point is locally asymptotically stable if and only if $R_0 < 1$.

3.8 Global Stability of Disease-free Equilibrium

Model(3) can be rewritten in the following form:

$$\begin{cases} \frac{dX}{dt} = H(X,Z), \\ \frac{dy}{dt} = G(X,Z), G(X,0) = 0. \end{cases} \tag{30}$$

The disease -free equilibrium E_0^1 of the preceding system is

$$E_0^1 = (X^0, 0, 0),$$

where X^0 is the disease-free equilibrium of the disease-free system.
According to [19] ,to guarantee global asymptotic stability,we verify the following conditions H_1 and H_2 to be satisfied:

i.H_1: for $\frac{dX}{dt} = H(X,0), X^0$ is the globally asymptotically stable equilibrium.
ii.H_2: $G(X,Z) = PY - \hat{G}(X,Z), \hat{G}(X,Z) \geq 0$ for $(X,Z) \in \Omega$.

Here,$P = D_Z G(X,0)$ satisfy the condition of the Metzler matrix, and Ω is a region of feasible solutions.
Now,we state the following theorem.

Theorem 7.*The disease-free equilibrium of the cholera dynamic model is globally asymptotically stable if $R_0 < 1$ if conditions H_1 and H_2 are satisfied and unstable whenever $R_0 > 1$.*

*Proof.*From model (3), we have

$$H(X,0) = \Pi - \mu S = H(S,0). \tag{31}$$

Solving $H(X,0) = 0$, we obtain $S = \frac{\Pi}{\mu}$.
Hence,$X^0 = (\frac{\Pi}{\mu}, 0)$.
Here, X^0 is the globally stable equilibrium of equation.

$$\frac{dX}{dt} = H(X,0). \tag{32}$$

From the infected compartments of model (3), we obtain;

$$G(X,Z) = \begin{bmatrix} -(\theta+\alpha_1+\mu+\xi) & 0 & 0 \\ \theta & -(\delta+\alpha_2+\mu+\xi) & 0 \\ \alpha_1 & \alpha_2 & r-\mu_B \end{bmatrix} \begin{bmatrix} I \\ Q \\ B \end{bmatrix} - \begin{bmatrix} -\frac{\beta_1 SB}{k+B} - \beta_2 SI \\ 0 \\ \frac{rB^2}{K} \end{bmatrix}.$$

At the disease -free equilibrium, the preceding equation reduces to the following form:

$$G(X,Z) = \begin{bmatrix} -(\theta+\alpha_1+\mu+\xi) & 0 & 0 \\ \theta & -(\delta+\alpha_2+\mu+\xi) & 0 \\ \alpha_1 & \alpha_2 & r-\mu_B \end{bmatrix} \begin{bmatrix} I \\ Q \\ B \end{bmatrix} - \begin{bmatrix} 0 \\ 0 \\ 0 \end{bmatrix}$$

$$G(X,Z) = PY - \hat{G}(X,Z),$$

Where

$$P = \begin{bmatrix} -(\theta+\alpha_1+\mu+\xi) & 0 & 0 \\ \theta & -(\delta+\alpha_2+\mu+\xi) & 0 \\ \alpha_1 & \alpha_2 & r-\mu_B \end{bmatrix} \text{ and } \hat{G}(X,Z) = \begin{bmatrix} 0 \\ 0 \\ 0 \end{bmatrix} \geq 0.$$

Now,it follows that the formulated model satisfied the hypothesis conditions required as,

$$G(X,Z) = PY - \hat{G}(X,Z),$$

where $\hat{G}(X,Z) \geq 0, \forall X,Z$.
Therefore, E_0 is globally asymptotically stable if $R_0 < 1$.

3.9 Global Stability of Endemic Equilibrium Point (EEP)

Theorem 8.*If $R_0 > 1$,then the endemic equilibrium point E^* of model (3) is globally asymptotically stable in the region Ω.*

*Proof.*Define a Lyapunov function candidate by;

$$F(S,I,Q,R) = \tfrac{1}{2}[(S-S^*)+(I-I^*)+(Q-Q^*)+(R-R^*)]^2.$$

Then $F(S,I,Q,R) \geq 0$ and $F(S^*,I^*,Q^*,R^*) = 0$. Moreover,

$$\tfrac{dF}{dt} = [(S+I+Q+R)-(S^*+I^*+Q^*+R^*)]\tfrac{dN}{dt}.$$

Since

$$S^*+I^*+Q^*+R^* = \tfrac{\Pi}{\mu}$$

and

$$\tfrac{dN}{dt} = \Pi - \mu N(t) - \alpha_1 I - \xi I - \alpha_2 Q - \xi Q,$$

we have

$$\tfrac{dF}{dt} = (N-\tfrac{\Pi}{\mu})(\Pi - \mu N(t) - \alpha_1 I - \xi I - \alpha_2 Q - \xi Q)$$
$$= -\tfrac{1}{\mu}(\Pi - \mu N)^2 - (\Pi - \mu N)(\alpha_1 I + \xi I + \alpha_2 Q + \xi Q) \leq 0.$$

Note that at the EEP we have $N \leq \frac{\Pi}{\mu}$. Hence,it follows that $\frac{dF}{dt}$ $leq0$ and $\frac{dF}{dt} = 0$ if and only if $S = S^*, I = I^*, Q = Q^*, R = R^*$. Therefore the largest closed and bounded invariant set in,

$$\left\{(S,I,Q,R,B) \in \Omega : \dot{F} = 0\right\}$$

is the set

$$\left\{E^* : E^* = (S^*,I^*,Q^*,R^*,B^*)\right\}.$$

By LaSalle's invariance principle the unique equilibrium point E^* is globally asymptotically stable when $R_0 > 0$ in the region Ω.

3.10 Bifurcation analysis

In this subsection, we establish the conditions on the parameters using Theorem 4.1 from [22] and center manifold theory [21]. In this theorem, there are two coefficients that represent dynamics on the center manifold. If we say these coefficients that 'decide' the bifurcation B_1 and B_2, we have $B_1 < 0$ and $B_2 > 0$ for the occurrence of forward bifurcation.
For the governing system (3), we will designate the effective cholera transmission rate, β_2, as the bifurcation parameter. Consequently, model (3) can be expressed in vector form by renaming the variables as follows:
$S = x_1, I = x_2, Q = x_3, R = x_4, B = x_5$. That is,

$$\frac{dX}{dt} = F(X). \tag{33}$$

Where, $X = (x_1,x_2,x_3,x_4,x_5)^T, F(X) = (f_1,f_2,f_3,f_4,f_5)$.
Then, model (3) becomes

$$\begin{cases} {}_0^C D_t^\alpha S(t) = \Pi - (\frac{\beta_1 SB}{k+B} + \beta_2 SI) - \mu S + \omega R = f_1, \\ {}_0^C D_t^\alpha I(t) = (\frac{\beta_1 SB}{k+B} + \beta_2 SI) - (\theta + \alpha_1 + \mu + \xi)I = f_2, \\ {}_0^C D_t^\alpha Q(t) = \theta I - (\delta + \alpha_2 + \mu + \xi)Q = f_3, \\ {}_0^C D_t^\alpha R(t) = \delta Q - (\omega + \mu)R = f_4, \\ {}_0^C D_t^\alpha B(t) = rB(1-\frac{B}{K}) + \alpha_1 I + \alpha_2 Q - \mu_B B = f_5. \end{cases} \tag{34}$$

Here, from preceding system of nonlinear equation, choosing β_2 as a bifurcation parameter and setting $R_0 = 1$, we have

$$\beta_2^* = \beta_2 = \frac{\mu}{\Pi m} - \frac{\beta_1\theta(-r+\mu_B)}{m^2\alpha_2 Kn} + \frac{\beta_1\alpha_1}{m\alpha_2 Kn}. \tag{35}$$

Where,$n=\theta+\alpha_1+\mu+\xi$ and $m=\delta+\alpha_2+\mu+\xi$.
So that the disease-free equilibrium, E_0, is locally stable when $\beta_2<\beta_2^*$ and is unstable when $\beta_2>\beta_2^*$. The linearized matrix of the system around the disease-free equilibrium E_0 and evaluated at β_2^* is given by

$$J(E_0,\beta_2^*)=\begin{bmatrix}-\mu & -\frac{\beta_2\Pi}{\mu} & 0 & \omega & \frac{-\beta_1\Pi}{\mu k}\\ 0 & \frac{\beta_2\Pi}{\mu}-(\theta+\alpha_1+\mu+\xi) & 0 & 0 & \frac{\beta_1\Pi}{\mu k}\\ 0 & \theta & -(\delta+\alpha_2+\mu+\xi) & 0 & 0\\ 0 & 0 & \delta & -(\omega+\mu) & 0\\ 0 & \alpha_1 & \alpha_2 & 0 & r-\mu_B.\end{bmatrix} \tag{36}$$

The system (36) with $\beta_2>\beta_2^*$ has a simple zero eigenvalues, hence the centre manifold theory will be used to analyse the dynamics of the system near $\beta_2=\beta_2^*$. The Jacobean matrix near $\beta_2=\beta_2^*$ has a right eigenvector associated with the zero eigenvalue given by, $w=(w_1,w_2,w_3,w_4,w_5)^T$ from the system;

$$J(E_0,\beta_2^*)w=\begin{bmatrix}-\mu & -\frac{\beta_2\Pi}{\mu} & 0 & \omega & \frac{-\beta_1\Pi}{\mu k}\\ 0 & \frac{\beta_2\Pi}{\mu}-(\theta+\alpha_1+\mu+\xi) & 0 & 0 & \frac{\beta_1\Pi}{\mu k}\\ 0 & \theta & -(\delta+\alpha_2+\mu+\xi) & 0 & 0\\ 0 & 0 & \delta & -(\omega+\mu) & 0\\ 0 & \alpha_1 & \alpha_2 & 0 & r-\mu_B\end{bmatrix}\begin{bmatrix}w_1\\w_2\\w_3\\w_4\\w_5\end{bmatrix}=\begin{bmatrix}0\\0\\0\\0\\0\end{bmatrix}.$$

The system of equation becomes

$$\begin{cases}-\mu w_1-\frac{\beta_2\Pi}{\mu}w_2+\omega w_4-\frac{\beta_1\Pi}{\mu K}w_5=0,\\ (\frac{\beta_2\Pi}{\mu}-(\theta+\alpha_1+\mu+\xi))w_2+\frac{\beta_1\Pi}{\mu K}w_5=0,\\ \theta w_2-(\delta+\alpha_2+\mu+\xi)w_3=0,\\ \delta w_3-(\omega+\mu)w_4=0,\\ \alpha_1 w_2+\alpha_2 w_3+(r-\mu_B)w_5=0.\end{cases} \tag{37}$$

After solving system of equation (37) we obtained

$$\begin{cases}w_1=\frac{\frac{\beta_2\Pi}{\mu}w_2+\omega w_4-\frac{\beta_1\Pi}{\mu K}w_5}{\mu},\\ w_2=w_2>0,\\ w_3=\frac{(\omega+\mu)w_4}{\delta},\\ w_4=w_4>0,\\ w_5=\frac{(\frac{\beta_2\Pi}{\mu}-(\theta+\alpha_1+\mu+\xi))w_2}{\frac{\beta_1\Pi}{\mu K}}.\end{cases} \tag{38}$$

The left eigenvectors of JE associated with the zero eigenvalue at $\beta_2=\beta_2^*$ is given by $v=(v_1,v_2,v_3,v_4,v_5)^T$, from the system (36),

$$J(E_0,\beta_2^*)v=\begin{bmatrix}-\mu & 0 & 0 & 0 & 0\\ -\frac{\beta_2\Pi}{\mu} & \frac{\beta_2\Pi}{\mu}-(\theta+\alpha_1+\mu+\xi) & \theta & 0 & \alpha_1\\ 0 & 0 & -(\delta+\alpha_2+\mu+\xi) & \delta & \alpha_2\\ \omega & 0 & 0 & -(\omega+\mu) & 0\\ \frac{-\beta_1\Pi}{\mu k} & \frac{\beta_1\Pi}{\mu k} & 0 & 0 & r-\mu_B\end{bmatrix}\begin{bmatrix}v_1\\v_2\\v_3\\v_4\\v_5\end{bmatrix}=\begin{bmatrix}0\\0\\0\\0\\0\end{bmatrix}.$$

$$\begin{cases}-\mu v_1=0,\\ -\frac{\beta_2\Pi}{\mu}v_1+(\frac{\beta_2\Pi}{\mu}-(\theta+\alpha_1+\mu+\xi))v_2+\theta v_3+\alpha_1 v_5=0,\\ -(\delta+\alpha_2+\mu+\xi)v_3+\delta v_4+\alpha_2 v_5=0,\\ \omega v_1-(\omega+\mu)v_4=0,\\ \frac{-\beta_1\Pi}{\mu k}v_1+\frac{\beta_1\Pi}{\mu k}v_2+(r-\mu_B)v_5.\end{cases} \tag{39}$$

Solving system of equation (39) gives

$$\begin{cases} v_1 = 0, \\ v_4 = 0, \\ v_3 = \frac{-\alpha_2 v_5}{(\delta+\alpha_2+\mu+\xi)} = 0, \\ v_5 = \frac{\frac{\beta_1 \Pi}{\mu k} v_2}{(r-\mu_B)}, \\ v_2 = v_2 > 0. \end{cases} \tag{40}$$

To study the stability of endemic equilibrium points, the center manifold theory is used to compute B_1 and B_2 such that,

$$B_1 = \sum_{k,j,i=1}^{n} v_k w_i w_j \frac{\partial^2 f}{\partial x_i \partial X_j}(S_o, 0, 0, 0, 0), \tag{41}$$

$$B_2 = \sum_{k,i=1}^{n} v_k w_i \frac{\partial^2 f}{\partial x_i \partial \beta_2^*}, \tag{42}$$

where

$$\begin{cases} \Pi - (\frac{\beta_1 x_1 x_5}{k+x_5} + \beta_2 x_1 x_2) - \mu x_1 + \omega x_4 = f_1, \\ (\frac{\beta_1 x_1 x_5}{k+x_5} + \beta_2 x_1 x_2) - (\theta + \alpha_1 + \mu + \xi) x_2 = f_2, \\ \theta x_2 - (\delta + \alpha_2 + \mu + \xi) x_3 = f_3, \\ \delta x_3 - (\omega + \mu) x_4 = f_4, \\ r x_5 (1 - \frac{x_5}{K}) + \alpha_1 x_2 + \alpha_2 x_3 - \mu_B x_5 = f_5. \end{cases} \tag{43}$$

We employ the center manifold theory as in [16] to compute the coefficients $B_i (i = 1, 2)$ in equation (27), thereby finalizing the bifurcation analysis. This involves determining the nonzero second-order partial derivatives of $f_k (k = 1, ..., 5)$ with respect to $x_i (i = 1, ..., 5)$ around the disease-free equilibrium.

The center manifold theory allows us to simplify the analysis of the dynamical system by reducing the dimension of the system around the bifurcation point. By computing the coefficients B_i, we can classify the type of bifurcation and predict the qualitative changes in the system's behavior as the bifurcation parameter, in this case the effective cholera transmission rate β_2 varies.

$$\begin{cases} \frac{\partial^2 f_1}{\partial x_1^2} =, \frac{\partial^2 f_1}{\partial x_1 \partial x_2} = \frac{\partial^2 f_1}{\partial x_2 \partial x_1} =, \frac{\partial^2 f_1}{\partial x_2^2} = \frac{\partial^2 f_1}{\partial x_4 \partial x_2} = \frac{\partial^2 f_1}{\partial x_2 \partial x_4} = 0, \frac{\partial^2 f_1}{\partial x_3 \partial x_2} = \frac{\partial^2 f_1}{\partial x_2 \partial x_3} = 0, \\ \frac{\partial^2 f_1}{\partial x_3^2} = \frac{\partial^2 f_1}{\partial x_1 \partial x_3} = \frac{\partial^2 f_1}{\partial x_3 \partial x_1} = \frac{\partial^2 f_1}{\partial x_4 \partial x_3} = \frac{\partial^2 f_1}{\partial x_3 \partial x_4} = \frac{\partial^2 f_1}{\partial x_4^2} = \frac{\partial^2 f_1}{\partial x_1 \partial x_4} = \frac{\partial^2 f_1}{\partial x_4 \partial x_1} = 0, \\ \frac{\partial^2 f_2}{\partial x_1^2} = \frac{\partial^2 f_2}{\partial x_1 \partial x_2} = \frac{\partial^2 f_2}{\partial x_2 \partial x_1} = \frac{\partial^2 f_2}{\partial x_2^2} = \frac{\partial^2 f_2}{\partial x_3 \partial x_2} = \frac{\partial^2 f_2}{\partial x_2 \partial x_3} = \frac{\partial^2 f_2}{\partial x_4 \partial x_2} = \frac{\partial^2 f_2}{\partial x_2 \partial x_4} = 0, \\ \frac{\partial^2 f_2}{\partial x_3^2} = \frac{\partial^2 f_2}{\partial x_1 \partial x_3} = \frac{\partial^2 f_2}{\partial x_3 \partial x_1} = \frac{\partial^2 f_2}{\partial x_4 \partial x_3} = \frac{\partial^2 f_2}{\partial x_3 \partial x_4} = \frac{\partial^2 f_2}{\partial x_4^2} = \frac{\partial^2 f_3}{\partial x_3 \partial x_2} = \frac{\partial^2 f_3}{\partial x_4 \partial x_2} = 0, \\ \frac{\partial^2 f_3}{\partial x_3^2} = \frac{\partial^2 f_3}{\partial x_4 \partial x_3} = \frac{\partial^2 f_3}{\partial x_1 \partial x_3} = \frac{\partial^2 f_2}{\partial x_1 \partial x_4} = \frac{\partial^2 f_2}{\partial x_4 \partial x_1} = \frac{\partial^2 f_3}{\partial x_1^2} = \frac{\partial^2 f_3}{\partial x_1 \partial x_2} = 0, \\ \frac{\partial^2 f_3}{\partial x_2^2} = \frac{\partial^2 f_3}{\partial f_4^2} = \frac{\partial^2 f_4}{\partial x_1 \partial x_4} = \frac{\partial^2 f_5}{\partial x_1^2} = \frac{\partial^2 f_5}{\partial x_1 \partial x_2} = \frac{\partial^2 f_5}{\partial x_2^2} = \frac{\partial^2 f_5}{\partial x_3 \partial x_2} = 0, \\ \frac{\partial^2 f_5}{\partial x_4 \partial x_2} = \frac{\partial^2 f_5}{\partial x_3^2} = \frac{\partial^2 f_5}{\partial x_1 \partial x_3} = \frac{\partial^2 f_5}{\partial x_4 \partial x_3} = \frac{\partial^2 f_5}{\partial x_4^2} = \frac{\partial^2 f_5}{\partial x_1 \partial x_4} = 0. \end{cases}$$

Also,

$$\begin{cases} \frac{\partial^2 f_2}{\partial x_2 \partial \beta_2^*}(E_0, \beta_2^*) = x_1, \\ \frac{\partial^2 f_3}{\partial x_3 \partial \beta_2^*}(E_0, \beta_2^*) = 0, \\ \frac{\partial^2 f_k}{\partial x_i \partial \beta_2^*}(E_0, \beta_2^*) = 0, i \neq 0. \end{cases}$$

Since $B_1 < 0$ and $B_2 > 0$, the model exhibits forward bifurcation at $R_0 = 1$.
Next, following procedures given in [13], we compute the bifurcation coefficients B_1 and B_2, to identify the direction of bifurcation at $R_0 = 1$. Thus, we have

$$\begin{cases} B_1 = \sum_{k,i,j=1}^{4} w_k v_i v_j \frac{\partial^2 f_k}{\partial x_i \partial x_j}(E_0, \beta_2^*) = \sum_{i,j=1}^{4} w_3 v_i v_j \frac{\partial^2 f_5}{\partial x_5 \partial x_5}(E_0, \beta_2^*) = \frac{-2}{(K} < 0, \\ B_2 = \sum_{k,i=1}^{4} w_k v_i \frac{\partial^2 f_k}{\partial x_i \partial \beta_2^*}(E_0, \beta_2^*) = w_2 v_2 \frac{\partial^2 f_2}{\partial x_2 \partial \beta_2^*}(E_0, \beta_2^*) = w_2 v_2 \frac{\partial^2 f_2}{\partial x_1 \partial \beta_2^*}(E_0, \beta_2^*) = w_2 v_2 x_1 \\ = w_2 v_2 \frac{\Pi}{\mu} = B_2 > 0. \end{cases} \tag{44}$$

Given that all parameters in model (1) are nonnegative, and additionally w_3 and v_3 are positive, we can deduce that $B_1 < 0$ and $B_2 > 0$. Consequently, following the findings of [9], model (3) demonstrates a supercritical bifurcation as R_0 crosses the threshold $R_0 = 1$. This implies the existence of a locally asymptotically stable endemic equilibrium point $E_1^* = (S^*, I^*, Q^*, R^*, B^*)$ for $R_0 > 1$. Drawing on the outcomes of the aforementioned discussion and referencing [10], the following theorem is formulated.

Theorem 9. *The trans-critical bifurcation of model (3) at $R_0 = 1$ is characterized as a supercritical bifurcation. This implies the presence of a locally asymptotically stable endemic equilibrium point $E_1 = (S^*, I^*, Q^*, R^*, B^*)$ for $R_0 > 1$.*

Remark. Theorem 10 indicates that when $R_0 > 1$, even a minor influx of infectious individuals into a fully susceptible population can lead to the sustained presence of cholera within the population.

3.11 Sensitivity Analysis and Its Interpretations

In this section we perform the sensitivity analysis of the reproductive number. Sensitivity analysis tells us how important each parameter is to disease transmission. Such information is crucial not only for experimental design, but also to data assimilation and reduction of complex nonlinear models. Sensitivity analysis is commonly used to determine the robustness of model predictions to parameter values, since there are usually errors in data collection and presumed parameter values. It is used to discover parameters that have a high impact on basic reproduction number and should be targeted by intervention strategies. The normalized forward sensitivity index of a particular variable, R_0, with respect to a parameter,ρ , is defined as

$$Y_\rho^{R_0} = \frac{\partial R_0}{\partial \rho} \times \frac{\rho}{R_0}$$

It is already shown that the explicit expression of R_0 is given by

$$R_0 = \frac{\beta_1 \Pi\theta(-r+\mu_B) + \beta_2 \Pi(\delta+\alpha_2+\mu+\xi)^2\alpha_2 K(\theta+\alpha_1+\mu+\xi) - \beta_1 \Pi\alpha_1(\delta+\alpha_2+\mu+\xi)}{\alpha_2\mu K(\theta+\alpha_1+\mu+\xi)(\delta+\alpha_2+\mu+\xi)}.$$

The normalized forward sensitivity indices of R_0 with respect to parameters in its are given as follows

$$\begin{cases} Y_{\beta_1}^{R_0} = \frac{\partial R_0}{\partial \beta_1} \times \frac{\beta_1}{R_0} = \frac{\theta\beta_1((\mu_B-r)-\alpha(\delta+\alpha_2+\mu+\xi))}{\beta_1\theta(\mu_B-r)+\beta_2(\delta+\alpha_2+\mu+\xi)^2\alpha_2 K(\theta+\alpha_1+\mu+\xi)-\beta_1\alpha_1(\delta+\alpha_2+\mu+\xi)}, \\ Y_{\Pi}^{R_0} = \frac{\partial R_0}{\partial \Pi} \times \frac{\Pi}{R_o} = 1, \\ Y_{\theta}^{R_0} = \frac{\partial R_0}{\partial \theta} \times \frac{\theta}{R_0} = \frac{\beta\theta((\mu_B-r)+\beta_2(\delta+\alpha_2+\mu+\xi)^2\alpha_2 K)}{\beta\theta(\mu_B-r)+\beta_2(\delta+\alpha_2+\mu+\xi)^2\alpha_2 K(\theta+\alpha_1+\mu+\xi)-\beta_1\alpha_1(\delta+\alpha_2+\mu+\xi)} - \frac{\theta}{\alpha\mu K(\delta+\alpha_2+\mu+\xi)}, \\ Y_{r}^{R_0} = \frac{\partial R_0}{\partial r} \times \frac{r}{R_0} = \frac{-\beta_1\theta r}{\beta_1\theta(\mu_B-r)+\beta_2(\delta+\alpha_2+\mu+\xi)^2\alpha_2 K(\theta+\alpha_1+\mu+\xi)-\beta_1\alpha_1(\delta+\alpha_2+\mu+\xi)}, \\ Y_{\mu_B}^{R_0} = \frac{\partial R_0}{\partial \mu_B} \times \frac{\mu_B}{R_0} = \frac{\beta_1\theta}{\beta_1\theta(\mu_B-r)+\beta_2(\delta+\alpha_2+\mu+\xi)^2\alpha_2 K(\theta+\alpha_1+\mu+\xi)-\beta_1\alpha_1(\delta+\alpha_2+\mu+\xi)}, \\ Y_{\beta_2}^{R_0} = \frac{\partial R_0}{\partial \beta_2} \times \frac{\beta_2}{R_0} = \frac{\beta_2\alpha_2 k(\delta+\alpha_2+\mu+\xi)^2(\theta+\alpha_1+\mu+\xi)}{\beta_1\theta(\mu_B-r)+\beta_2(\delta+\alpha_2+\mu+\xi)^2\alpha_2 K(\theta+\alpha_1+\mu+\xi)-\beta_1\alpha_1(\delta+\alpha_2+\mu+\xi)}, \\ Y_{\alpha_1}^{R_0} = \frac{\partial R_0}{\partial \alpha_1} \times \frac{\alpha_1}{R_0} = \frac{\beta_2\alpha_2 k(\delta+\alpha_2+\mu+\xi)^2 K\alpha_1}{\beta_1\theta(\mu_B-r)+\beta_2(\delta+\alpha_2+\mu+\xi)^2\alpha_2 K(\theta+\alpha_1+\mu+\xi)-\beta_1\alpha_1(\delta+\alpha_2+\mu+\xi)} - \frac{\alpha_1}{\alpha_2\mu K(\delta+\alpha_2+\mu+\xi)(\theta+\alpha_1+\mu+\xi)}, \\ Y_{\alpha_2}^{R_0} = \frac{\partial R_0}{\partial \alpha_2} \times \frac{\alpha_2}{R_0} = \frac{\beta_2\xi(\theta+\alpha_1+\mu+\xi)k(\delta+2\alpha_2+\mu+\xi)-\beta\alpha_1\alpha_2}{\beta_1\theta(\mu_B-r)+\beta_2(\delta+\alpha_2+\mu+\xi)^2\alpha_2 K(\theta+\alpha_1+\mu+\xi)-\beta_1\alpha_1(\delta+\alpha_2+\mu+\xi)} - \frac{(\delta+2\alpha_2+\mu+\xi)\mu K\alpha_2(\theta+\alpha_1+\mu+\xi)}{\alpha\mu K(\theta+\alpha_1+\mu+\xi)(delta+\alpha_2+\mu+\xi)}, \\ Y_{\delta}^{R_0} = \frac{\partial R_0}{\partial \delta} \times \frac{\delta}{R_0} = \frac{(2\beta_2(delta+\alpha_2+\mu+\xi)\alpha_2 K(\theta+\alpha_1+\mu+\xi))\delta}{\beta_1\theta(\mu_B-r)+\beta_2(\delta+\alpha_2+\mu+\xi)^2\alpha_2 K(\theta+\alpha_1+\mu+\xi)-\beta_1\alpha_1(\delta+\alpha_2+\mu+\xi)} - \frac{\delta}{(\delta+\alpha_2+\mu+\xi)}, \\ Y_{\xi}^{R_0} = \frac{\partial R_0}{\partial \xi} \times \frac{\xi}{R_0} = \frac{\beta_2\alpha_2 K\xi(\delta+\alpha_2+\mu+\xi)^2}{\beta_1\theta(\mu_B-r)+\beta_2(\delta+\alpha_2+\mu+\xi)^2\alpha_2 K(\theta+\alpha_1+\mu+\xi)-\beta_1\alpha_1(\delta+\alpha_2+\mu+\xi)} - \frac{\delta}{(\delta+\alpha_2+\mu+\xi)} - \frac{\xi}{(\theta+\alpha_1+\mu+\xi)}. \end{cases}$$

where,
$P = \beta_1 \Pi \theta(-r+\mu_B) + \beta_2 \Pi m^2 \alpha_2 Kn - \beta_1 \Pi \alpha_1 m$,
$m = \delta + \alpha_2 + \mu + \xi$,
$n = \theta + \alpha_1 + \mu + \xi$.

Table 1: Sensitivity Indices Table

Parameters Symbol	Description	Sensitivity indices
Π	Recruitment rate into the human population	1
ξ	Cholera induced death rate	0.654
δ	Rate of recovery using the available cholera treatment from $Q(t)$	0.437
α_2	Rate of contribution from $Q(t)$ to $B(t)$	0.365
β_1	Ingestion rate	0.235
r	Intrinsic growth rate	0.0002
θ	Rate of infected individuals join $Q(t)$ class	-0.125
β_2	Transmission rate	-0.136
α_1	Rate of contribution from $I(t)$ to $B(t)$	-0.459
μ_B	Bacteria removal rate	-0.812

The sensitivity analysis interpretation of our basic reproduction number is described as follows. The parameters that have negative sensitivity indices $(\beta_2, \theta, \alpha_1, \mu_B))$ have the effect of reducing the burden of cholera from the community if the values of the parameters are decreasing (which means that the basic reproduction number of the disease decreases as their parameter values decrease) by keeping other parameter constant. Also, those parameters with positive sensitivity indices $(\xi, \delta, \alpha_2, \beta_1, r)$ have an important role in the expansion of Cholera in the community if their values increase (this means that if their parameter values increase, then the secondary infection in the community increases). Due to the reason that R_0 (effective reproductive number) increases as its parameter cost will increase, the common wide variety of secondary contamination will increase withinside the population; and R_0 decreases as its parameter value decreases, which means that the average number of secondary contamination decreases withinside the human population and illustrated as Figure (2).

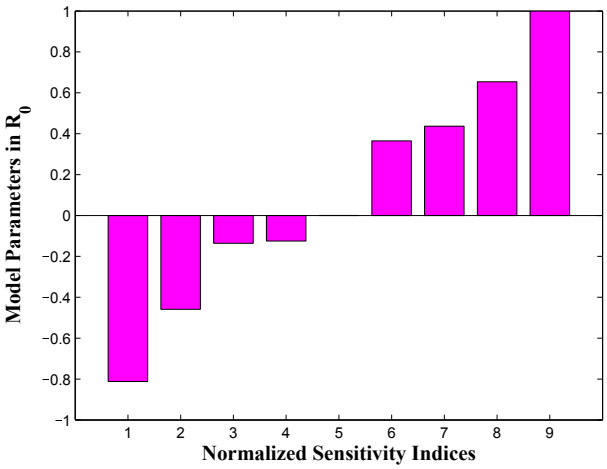

Fig. 2: Sensitivity indices of basic reproduction number R_0

4 Optimal Control Model

The aim of this section is to extend model equation (1) into an optimal control problem. The controls are defined as follows;

i)$u_1(t)$ a prevention effort that protect susceptible individuals from contracting the disease and Vibrio cholerae.
ii)$u_2(t)$ a treatment for cholera-infected individuals through quarantine , with $0 \leq u_2(t) \leq 1$ [14].
iii)$u_3(t)$ is a water sanitation , with

$$0 \leq u_3(t) \leq 0.1$$

[17].

After in corporating the controls , the corresponding state system for model equation (1) is given as ;

$$\begin{cases} \frac{dS}{dt} = \Pi - (1-u_1(t))(\frac{\beta_1 SB}{k+B} + \beta_2 SI) - \mu S + \omega R, \\ \frac{dI}{dt} = (1-u_1(t))(\frac{\beta_1 SB}{k+B} + \beta_2 SI) - (\theta + \alpha_1 + \mu + \xi + u_2(t))I, \\ \frac{dQ}{dt} = \theta + u_2(t)I - (\delta + \alpha_2 + \mu + \xi)Q, \\ \frac{dR}{dt} = \delta Q - (\omega + \mu)R, \\ \frac{dB}{dt} = u_3(t)rB(1 - \frac{B}{K}) + \alpha_1 I + \alpha_2 Q - \mu_B B. \end{cases} \tag{45}$$

With initial condition

$$S(0) > 0, I(t) \geq 0, Q(t) \geq 0, R(t) \geq 0, B(t) \geq 0.$$

and a bounded lebesgue measurable control set .

4.1 Construction of Objective Function

Although L^1 type cost function is more robust than L^2 type cost function, most papers done on optimal control problems adopt L^2 type cost function aim for a simply calculations [15]. In this subsection we apply L^2 type cost function to define the objective functional J that describes the optimal level of effort required to control cholera infection. Moreover, the aim of objective functional is to minimize the number of infected humans $I(t)$, the concentrations of Vibrio cholerae in the environment $B(t)$,the quarantine human and the cost of providing and applying the controls u_1, u_2 and u_3. Here, similar to the works done in [5], we choose the quadratic cost on controls. Thus, under these control measures, we consider the following optimal control problem:

$$J(I,U,t) = min_{u_1,u_2,u_3} \int_0^{t_f} M_1 I + M_2 B + M_3 Q + \frac{1}{2}(\sum_{i=1}^{3} w_i u_i^2)dx, \tag{46}$$

subject to the control system

$$\begin{cases} \frac{dS}{dt} = \Pi - (1-u_1(t))(\frac{\beta_1 SB}{k+B} + \beta_2 SI) - \mu S + \omega R, \\ \frac{dI}{dt} = (1-u_1(t))(\frac{\beta_1 SB}{k+B} + \beta_2 SI) - (\theta + \alpha_1 + \mu + \xi + u_2(t))I, \\ \frac{dQ}{dt} = (\theta + u_2(t))I - (\delta + \alpha_2 + \mu + \xi)Q, \\ \frac{dR}{dt} = \delta Q - (\omega + \mu)R, \\ \frac{dB}{dt} = u_3(t)rB(1 - \frac{B}{K}) + \alpha_1 I + \alpha_2 Q - \mu_B B. \end{cases} \tag{47}$$

Where $i = 1,2,3$ and M_1, M_2, M_3, $\frac{w_1}{2}$, $\frac{w_2}{2}$ and $\frac{w_3}{2}$ are positive weights that balance the size of the integrand terms to reduce the dominance of any of the term in the integral. The constants M_1 , M_2 and M_3 measures the cost or effort required for the implementation of each of the three control measures adopted while u_1, u_1 and u_3 measures the relative importance of reducing the associated classes on the spread of the disease.The parameter T is the duration of time in years of prevention and treatment progress. Thus, we need to find the optimal controls
$u^* = (u_1^*, u_2^*, u_3^*)$ such that;
$J(u^*) = min_u J(u_1, u_2, u_3)$
Hence, the basic setup of the optimal control problem is to check the existence and uniqueness of the optimal controls and to characterize them.

4.2 Existence of an Optimal Control

Theorem 10.*Consider the objective function J(u) as (46) with the set of admissible control Ω subject to the system ,then there exist an optimal control $(u_1^*, u_2^*, u_3^*) \in \Omega$ such that*

$$J(u_1^*, u_2^*, u_3^*) = min(u_1, u_2, u_3^* \in \Omega) J(u_1, u_2, u_3^*)$$

the subsequent situations are satisfied.

Let the control set

$$u = [0,1]^2, \upsilon = (u_1, u_2, u_3^*) \in u, \chi = (S^*, I^*, Q^*, R^*, B^*)$$

and $f(t, \chi, \upsilon)$ the right hand side of state system (46), is given by

$$f(t,\chi,\upsilon) = \begin{cases} \frac{dS}{dt} = \Pi - (1-u_1(t))(\frac{\beta_1 SB}{k+B} + \beta_2 SI) - \mu S + \omega R, \\ \frac{dI}{dt} = (1-u_1(t))(\frac{\beta_1 SB}{k+B} + \beta_2 SI) - (\theta + \alpha_1 + \mu + \xi + u_2(t))I, \\ \frac{dQ}{dt} = (\theta + u_2(t))I - (\delta + \alpha_2 + \mu + \xi)Q, \\ \frac{dR}{dt} = \delta Q - (\omega + \mu)R, \\ \frac{dB}{dt} = u_3(t) rB(1 - \frac{B}{K}) + \alpha_1 I + \alpha_2 Q - \mu_B B. \end{cases} \tag{48}$$

The proof is based on the following assumption and by Fleming and Rishel's theorem.

1.The set of controls and corresponding state variables is nonempty.
2.The admissible control set Ω is convex and closed.
3.All the right hand sides of equations of system (1) are continuous, bounded above by a sum of bounded control and state, and can be written as a linear function of u, v and w with coefficients depending on time and state.
4.The integrand of the objective functional $M_1 I + M_2 B + M_3 Q + \frac{1}{2} w_1 u_1^2 + \frac{1}{2} w_2 u_2^2 + \frac{1}{2} w_3 u_3^2$ is convex.
5.The integrand of the objective functional is bounded below by

$$M_1 I + M_2 B + + M_3 Q + \tfrac{1}{2} w_1 u_1^2 + \tfrac{1}{2} w_2 u_2^2 + \tfrac{1}{2} w_3 u_3^2 \geq c_1 + c_2 |u_1|^\tau + c_3 |u_2|^\tau + c_4 |u_3|^\tau.$$

where $c_1, c_2, c_3, c_4 > 0$ and $\tau > 1$.

*Proof.*The non trivial requirement on the set of admissible controls and the set of end conditions are followed by[2] theorem.
Condition 1: Using theorem 3.2 of Picard-Lindelof, if $g(t, \chi, \upsilon)$ is bounded, continuous and Lipschitz in the state variables, then there exists a unique solution corresponding to every admissible control Ω. Hence, for every $u_i \in \Omega$ and the state variables, we have

$$0 \leq N(t) \leq \frac{\Pi}{\mu}, B(t) \leq \frac{(\alpha_1 + \alpha_2)}{\mu \mu_B r} \Pi K. \tag{49}$$

and non empty by model assumption. Furthermore, with the bounded done in (10) it implies that the state variable is continuous and bounded. Additionally, the partial derivative $\frac{\partial f}{\partial x}$ exist and finite (i.e. are all continuous). Therefore, there exists a unique solution (S, I, Q, R, B) that satisfies the initial conditions. Hence, the set of controls and the corresponding state variables is nonempty and condition 1 is satisfied.
Condition 2: Assume that
$\Omega = \{u \in \Re^3 : ||u|| \leq 1 - \varepsilon\}$. Let $u_1, u_2 \in \Omega$ such that $||u_1|| \leq 1 - \varepsilon$ and $||u_2|| \leq 1 - \varepsilon$. Then for any $\rho \in [0,1]$,

$$||\rho u_1 + (1-\rho)u_2|| \leq \rho ||u_1|| + (1-\rho)||u_2|| \leq 1 - \varepsilon.$$

This implies that Ω is convex and closed.
The existence of the result in (10) for the equation of system (1) with bounded coefficients is used to hold the condition under (2). The control set u is convex and is closed by definition. The RHS of the state variables in (1) holds. Condition (10) as the state solutions is a priori bounded. The integrand of the objective functional $M_1 I + M_2 B + M_3 Q + \frac{1}{2} \sum_{i=1}^{2} w_i u_i^2(t)$ is clearly concave on u. Finally, $n_1 > 0, n_2 > 0$ and $\beta > 0$.

$$M_1 I + M_2 B + M_3 Q + \frac{1}{2} \sum_{i=1}^{2} w_i u_i^2(t) \leq n_1 - n_2 (u_1^2, u_2^2, u_3^2)^{\frac{\alpha}{2}}. \tag{50}$$

The state variables are bounded. Hence, there exists an optimal control (u_1, u_2, u_3) that minimizes the objective functional $J(u_1, u_2, u_3)$.

4.3 Construction of Hamiltonian Function

The necessary condition that an optimal control must satisfy comes from Pontryagin's Maximum Principle [1]. The principle converts equations of objective functional into a problem of minimizing point wise a Hamiltonian H, with respect to the controls u_1, u_2, and u_3. Let $\lambda_1, \lambda_2, \lambda_3, \lambda_4$ and λ_5 be the adjoint variables with respect to state variables S, I, Q, R and B, respectively. Then Hamiltonian function can be constructed as follows:

$$H = M_1 I + M_2 B + M_3 Q + \frac{1}{2} w_1 u_1^2 + \frac{1}{2} w_2 u_2^2 + \frac{1}{2} w_3 u_3^2 + \lambda_1 \frac{dS}{dt} + \lambda_2 \frac{dI}{dt} + \lambda_3 \frac{dQ}{dt} + \lambda_4 \frac{dR}{dt} + \lambda_5 \frac{dB}{dt}.$$

With conditions:

1. $\frac{d\lambda_1}{dt} = -\frac{\partial H}{\partial S}, \frac{d\lambda_2}{dt} = -\frac{\partial H}{\partial I}, \frac{d\lambda_3}{dt} = -\frac{\partial H}{\partial Q}, \frac{d\lambda_4}{dt} = -\frac{\partial H}{\partial R}, \frac{d\lambda_5}{dt} = -\frac{\partial H}{\partial B}$
2. $\frac{\partial H}{\partial u_1} = 0, \frac{\partial H}{\partial u_2} = 0, \frac{\partial H}{\partial u_3} = 0.$

4.4 Characterization of optimal control solution

According to Pontryagin's minimum principle (22), and using the results described in [4], if $u^* \in \Omega$is optimal solution for the objective functional (21), then there exists an adjoint vector $\lambda = (\lambda_{S(t)}, \lambda_{I(t)}, \lambda_{Q(t)}, \lambda_{R(t)}, \lambda_{B(t)}) \in R_+^5$ satisfies:

(i)the control system

$$\begin{cases} \frac{d\lambda_1}{dt} = -\frac{\partial H}{\partial S}, \\ \frac{d\lambda_2}{dt} = -\frac{\partial H}{\partial I}, \\ \frac{d\lambda_3}{dt} = -\frac{\partial H}{\partial Q}, \\ \frac{d\lambda_4}{dt} = -\frac{\partial H}{\partial R}, \\ \frac{d\lambda_5}{dt} = -\frac{\partial H}{\partial B}. \end{cases} \tag{51}$$

(ii)the adjoint system

$$\frac{d\lambda_1}{dt} = -\frac{\partial H}{\partial S}, \frac{d\lambda_2}{dt} = -\frac{\partial H}{\partial I}, \frac{d\lambda_3}{dt} = -\frac{\partial H}{\partial Q}, \frac{d\lambda_4}{dt} = -\frac{\partial H}{\partial R}, \frac{d\lambda_5}{dt} = -\frac{\partial H}{\partial B}; \tag{52}$$

(iii)the stationary condition

$$\frac{\partial H}{\partial u_1} = 0, \frac{\partial H}{\partial u_2} = 0, \frac{\partial H}{\partial u_3} = 0; \tag{53}$$

(iv)the transversality conditions

$$\lambda_{S(t_f)} = 0, \lambda_{I(t_f)} = 0, \lambda_{Q(t_f)} = 0, \lambda_{R(t_f)} = 0, \lambda_{B(t_f)} = 0; \tag{54}$$

in which the Hamiltonian function is defined as
$H = M_1 I + M_2 B + M_3 Q + \frac{1}{2} w_1 u_1^2 + \frac{1}{2} w_2 u_2^2 + \frac{1}{2} w_3 u_3^2 + \lambda_1 \frac{dS}{dt} + \lambda_2 \frac{dI}{dt} + \lambda_3 \frac{dQ}{dt} + \lambda_4 \frac{dR}{dt} + \lambda_5 \frac{dB}{dt}.$

Theorem 11. *Let $(S^*, I^*, Q^*, R^*, B^*)$ be optimal state variables set related to optimal control solution $U^* = (u_1^*, u_2^*, u_3^*)$ which minimizes the objective function for the optimal control problem (21)-(22), then there exists an adjoint variable $\lambda = (\lambda_S, \lambda_I, \lambda_Q, \lambda_R, \lambda_B)$ satisfying*

$$\begin{cases} \frac{d\lambda_1}{dt} = \lambda_1[(1-u_1)\frac{\beta_1 B}{k+B} + \beta_2 I + \mu] - \lambda_2(1-u)(\frac{\beta_1 B}{k+B} + \beta_2 I), \\ \frac{d\lambda_1}{dt} = \lambda_1((1-u_1)\beta_2 S) - \lambda_2(1-u_1)\beta_2 S + \lambda_2(\theta + \alpha_1 + \mu + \xi + u_2) - \lambda_3(\theta + u_2) - \lambda_5 \alpha_1, \\ \frac{d\lambda_3}{dt} = \lambda_3(\delta + \alpha_2 + \mu + \xi) - \lambda_4 \delta - \lambda_5 \alpha_2, \\ \frac{d\lambda_4}{dt} = -\lambda_1 \omega + \lambda_3(\omega + \mu), \\ \frac{d\lambda_5}{dt} = \lambda_1((1-u_1)(\frac{\beta_1 S(k+B) - \beta_1 SB}{(k+B)^2})) - \lambda_2((1-u_1)(\frac{\beta_1 S(k+B) - \beta_1 SB}{(k+B)^2})) - \lambda_5(u_3 r - \frac{2u_3 rB}{K} - \mu_B). \end{cases} \tag{55}$$

And with transversality conditions,

$$\lambda_{1(t_f)} = 0, \lambda_{2(t_f)} = 0, \lambda_{3(t_f)} = 0, \lambda_{4(t_f)} = 0, \lambda_{5(t_f)} = 0. \tag{56}$$

$$\begin{cases} u_1^* = min\left\{max\left\{0, \frac{(\lambda_1-\lambda_2)(\frac{\beta_1 SI}{k+B}+\beta_2 SI)}{w_1}\right\}, u_1 max\right\}, \\ u_2^* = min\left\{max\left\{0, \frac{(\lambda_2-\lambda_3)I}{w_2}\right\}, u_2 max\right\}, \\ u_3^* = min\left\{max\left\{0, -\frac{\lambda_5 rB(1-\frac{B}{K})}{w_3}\right\}, u_3 max\right\}. \end{cases} \tag{57}$$

Therefore, we obtain the optimal controls and states by solving the optimal system which includes the state system with initial conditions, the adjoint system, and the characterization of the optimal controls. Thus, substituting optimal controls $u_1^*(t), u_2^*(t)$, and $u_3^*(t)$ in the control model equations, we arrived at the optimality system.

$$\begin{cases} \frac{dS}{dt} = \Pi - (1-u_1(t))(\frac{\beta_1 SB}{k+B} + \beta_2 SI) - \mu S + \omega R, \\ \frac{dI}{dt} = (1-u_1(t))(\frac{\beta_1 SB}{k+B} + \beta_2 SI) - (\theta + \alpha_1 + \mu + \xi + u_2(t))I, \\ \frac{dQ}{dt} = (\theta + u_2(t))I - (\delta + \alpha_2 + \mu + \xi)Q, \\ \frac{dR}{dt} = \delta Q - (\omega + \mu)R, \\ \frac{dB}{dt} = u_3(t)rB(1-\frac{B}{K}) + \alpha_1 I + \alpha_2 Q - \mu_B B, \\ \frac{d\lambda_1}{dt} = \lambda_1[(1-u_1)\frac{\beta_1 B}{k+B} + \beta_2 I + \mu] - \lambda_2(1-u)(\frac{\beta_1 B}{k+B} + \beta_2 I), \\ \frac{d\lambda_1}{dt} = \lambda_1((1-u_1)\beta_2 S) - \lambda_2(1-u_1)\beta_2 S + \lambda_2(\theta + \alpha_1 + \mu + \xi + u_2) - \lambda_3(\theta + u_2) - \lambda_5\alpha_1, \\ \frac{d\lambda_3}{dt} = \lambda_3(\delta + \alpha_2 + \mu + \xi) - \lambda_4\delta - \lambda_5\alpha_2, \\ \frac{d\lambda_4}{dt} = -\lambda_1\omega + \lambda_3(\omega + \mu), \\ \frac{d\lambda_5}{dt} = \lambda_1((1-u_1)(\frac{\beta_1 S(k+B)-\beta_1 SB}{(k+B)^2})) - \lambda_2((1-u_1)(\frac{\beta_1 S(k+B)-\beta_1 SB}{(k+B)^2})) - \lambda_5(u_3 r - \frac{2u_3 rB}{K} - \mu_B). \end{cases} \tag{58}$$

With initial conditions: $S(0) > 0$, $I(0) \geq 0$, $Q(0) \geq 0$,$R(0) \geq 0$ and $B(0) \geq 0$ Transversality conditions: $\lambda_1(t_f) = \lambda_2(t_f) = \lambda_3(t_f) = \lambda_4(t_f) = \lambda_5(t_f) = 0$ and control conditions: $0 \leq u_1 \leq 1$, $0 \leq u_2(t) \leq 1$, and $0 \lesssim u_3 \lesssim 1$. Moreover, the controls u_i are in function of time t. Also, due to the boundedness of the state and adjoint variables, the optimality system has unique solution for small time t_f.

Table 2: Parameters in model and their descriptions in model

Symbols	Parameters	Initial values	Reference
β_1	rate of transmission from environment to human	0.001	Assumed
β_1	rate of transmission from human to human	0.5	Assumed
μ	rate of natural death	0.001	[23]
ω	rate of recovered individuals who lose immunity	0.05	[23]
k	Concertaration of vibrios cholera	10^6	[23]
θ	rate of infection	0.03	[4,5]
α_1	rate of contribution from $I(t)$	0.09	Assumed
ξ	Induced death rate	20	[23]
δ	rate of recover as a result of cholera treatment	0.33	[23]
α_2	rate of contribution from $Q(t)$	0.007	Estimated
r	intrinsic growth rate	0.004	Estimated
K	carrying capacity	200	Estimated
μ_B	bacterial removal rate	0.006	Estimated

5 Numerical Results and Discussion

5.1 Numerical simulation I

The objective of this section is to explain the impact of different values of fractional order α in model (3). To this end, we give several numerical simulations of the model using the MATLAB software. The parameters presented in Table 2

are used in the simulation of solutions of SIQR-B model and are either assumed or taken from the literature and and the initial conditions $S(0) = 9000, I(0) = 6000, Q(0) = 4000, R(0) = 1000, B(0) = 1200$ in the model equations (3) and a simulation study is conducted and the results are given in the following Figures. In Fig.2, the memory effect is displayed by considering the level of impacts imposed. The more the memory impact considered, the more the possibility to influence the growth of V. cholerae in the environment. The high-order of fractional derivative value indicates more impacts on the growth of V. cholerae. In Figure 2, the order of fractional derivative shows the influence of memory effect on cholera recovered individuals. The more the memory effect on the community, the more individuals shows cholera recovered with immunity. In Figure 3, the impact of memory effect on cholera recovered individuals is illustrated. Cholera infected individuals decrease when the order of fractional derivative is more. The memory effect on individuals descend the number of individuals who become infected with cholera disease.

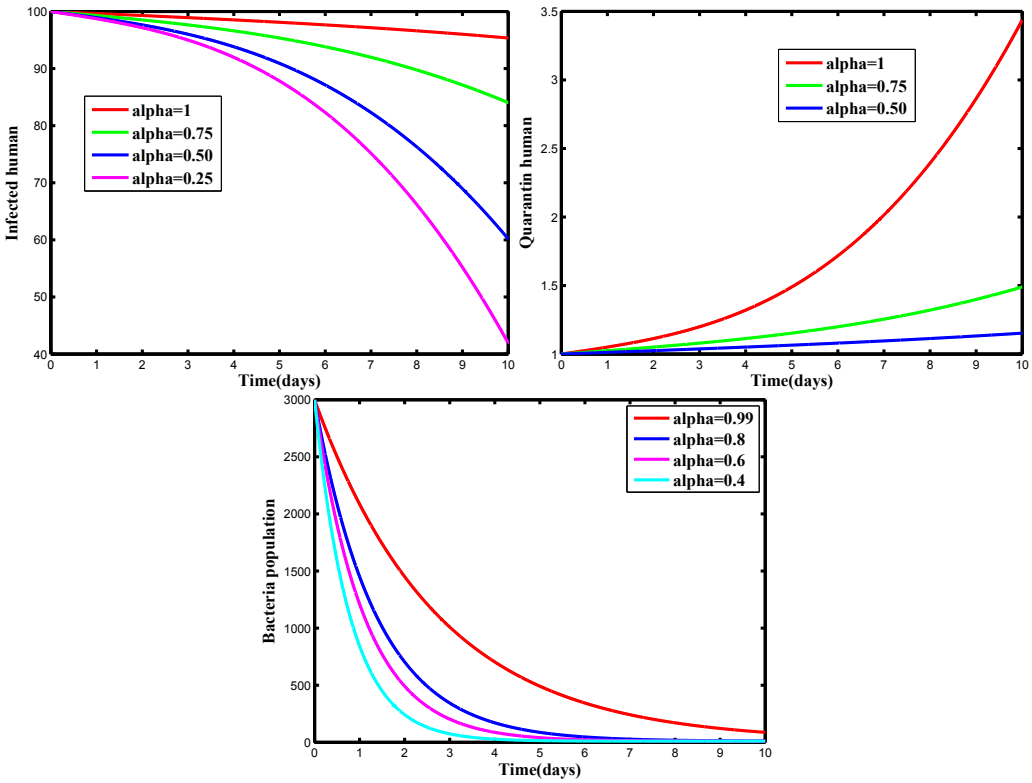

Fig. 3: (a) Effects of memory (order of derivatives) (alpha) on I. (b) Effects of memory (order of derivatives) (alpha) on Q. (c) Effects of memory (order of derivatives) (alpha) on B.

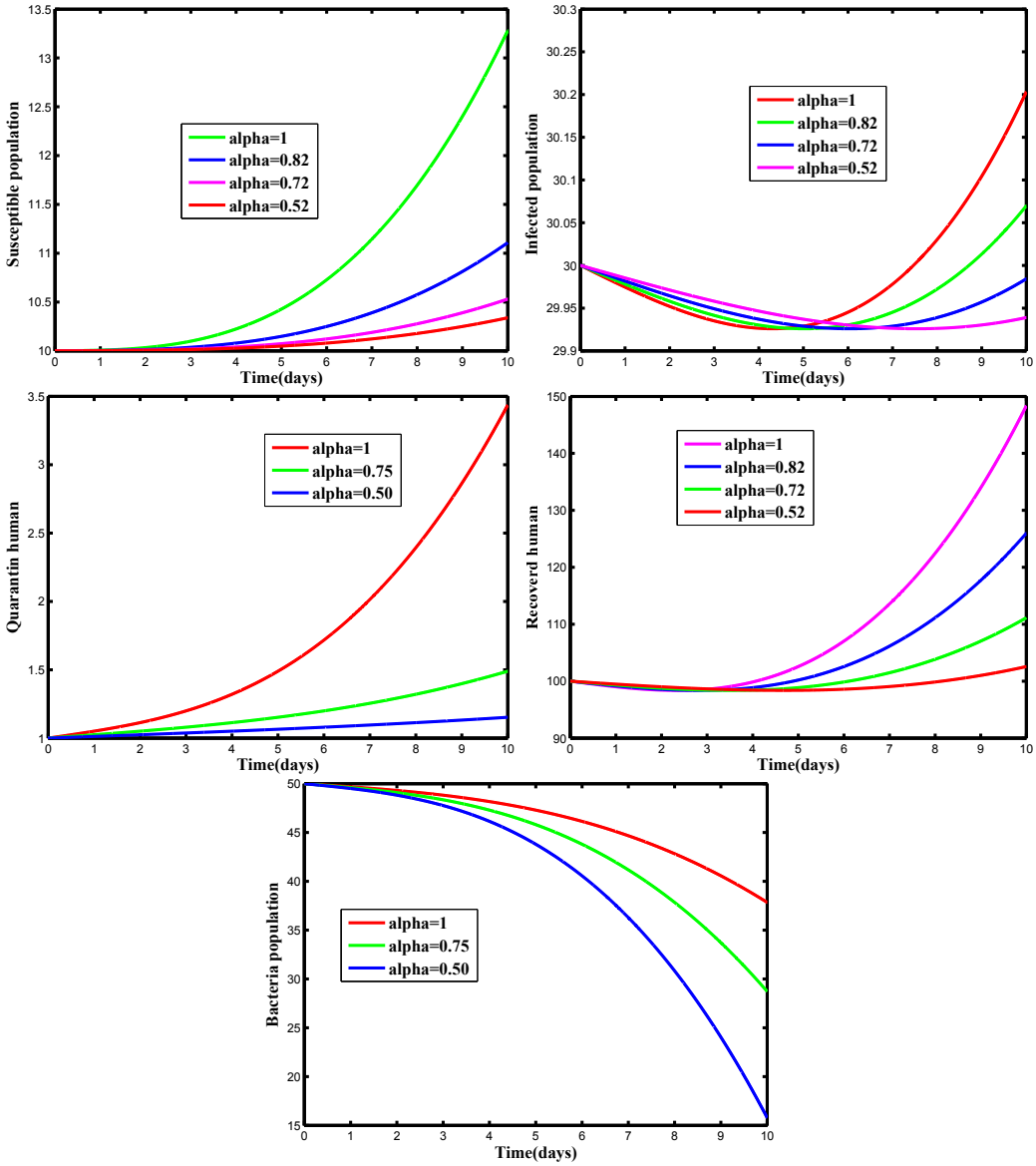

Fig. 4: Caputo fractional-order dynamical behavior of each state variable

5.2 Numerical simulation II

Using different combinations of the controls such as one control only at a time and also all controls at a time, that we analyse and compare numerical results from simulations with the following scenarios. Moreover, the applied control strategies are described as follows:

1.Strategy 1: apply combination of prevention and treatment of effected human
2.Strategy 2: apply combination of prevention and sanitation of water
3.Strategy 3: apply combination of treatment of effected human and sanitation of water
4.Strategy 4: apply combination of prevention, treatment of effected human and sanitation of water

The optimal control problem is obtained by solving the optimality system. We used fourth-order Runge-Kutta's methods, both forward and backward methods were used to analyses the optimality problem. The details of control strategy are described as follows:

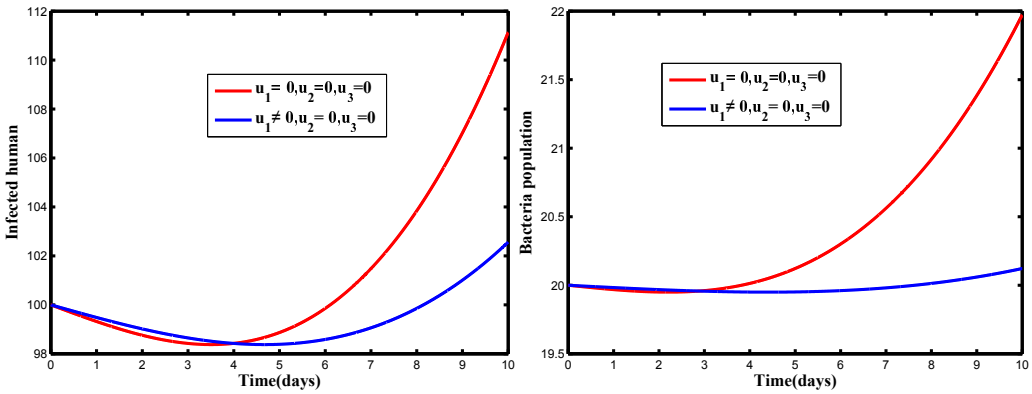

Fig. 5: Simulations of optimality system with prevention only.

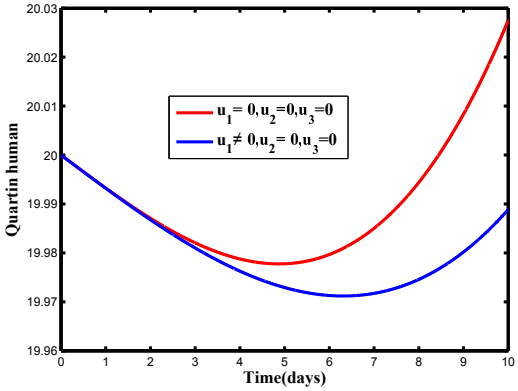

Fig. 6: Simulations of optimality system with prevention only.

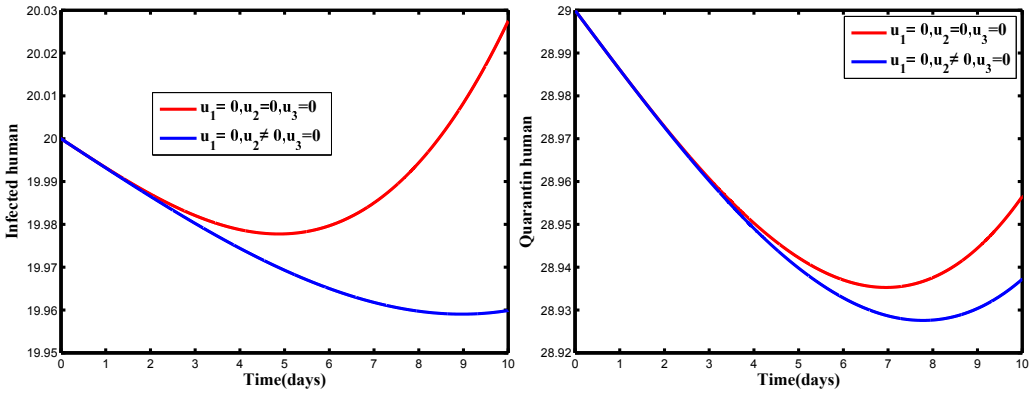

Fig. 7: Simulations of optimality system with treatment only.

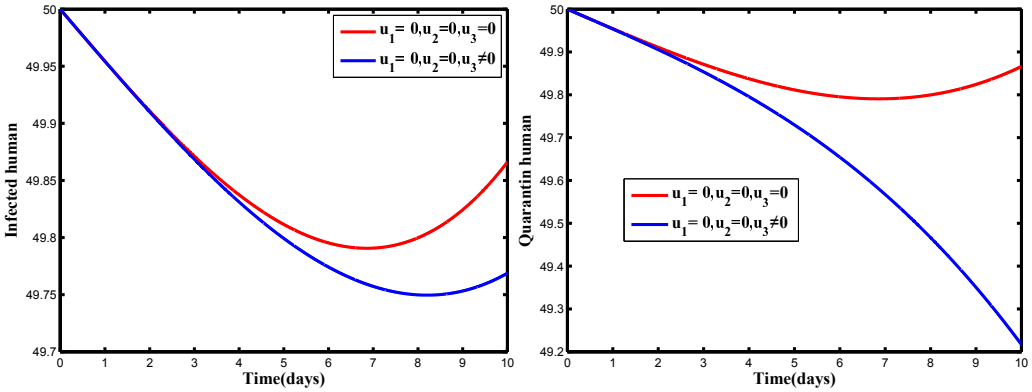

Fig. 8: Simulations of optimality system with water sanitation only.

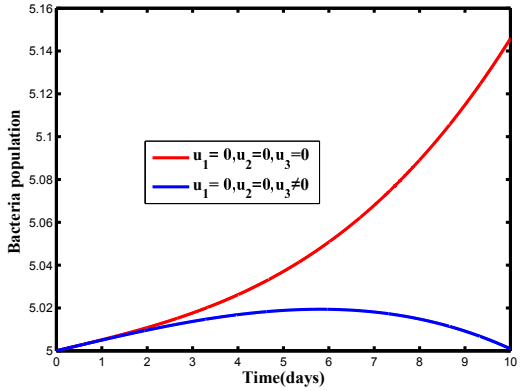

Fig. 9: Simulations of optimality system with water sanitation only.

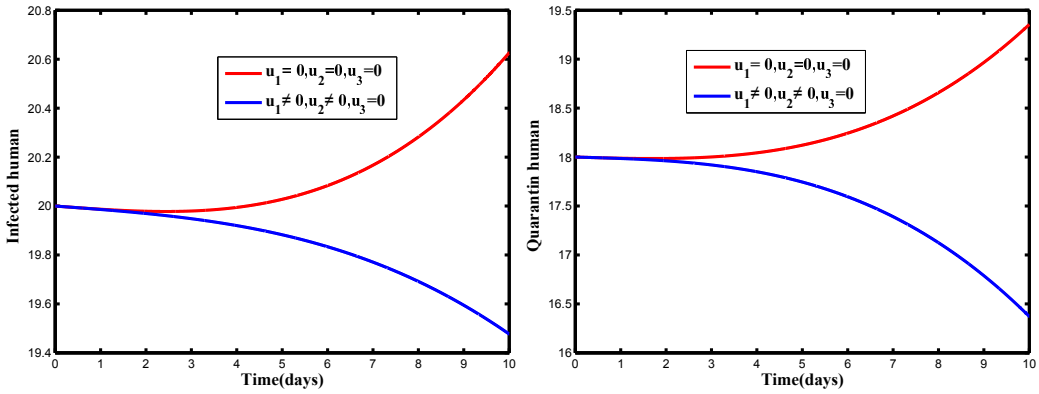

Fig. 10: Simulations of optimality system with prevention and treatment.

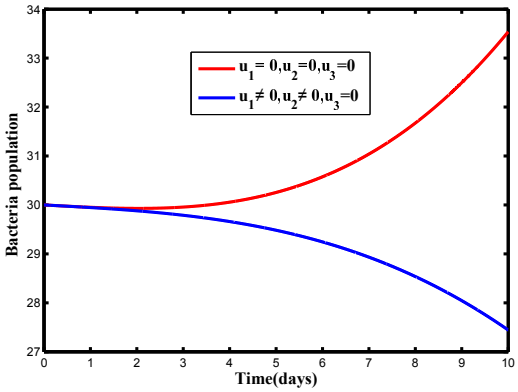

Fig. 11: Simulations of optimality system with prevention and treatment.

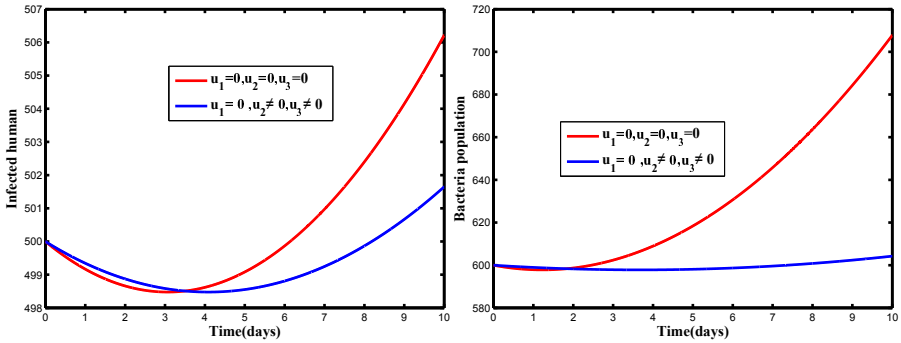

Fig. 12: Simulation of treatment and water sanitation

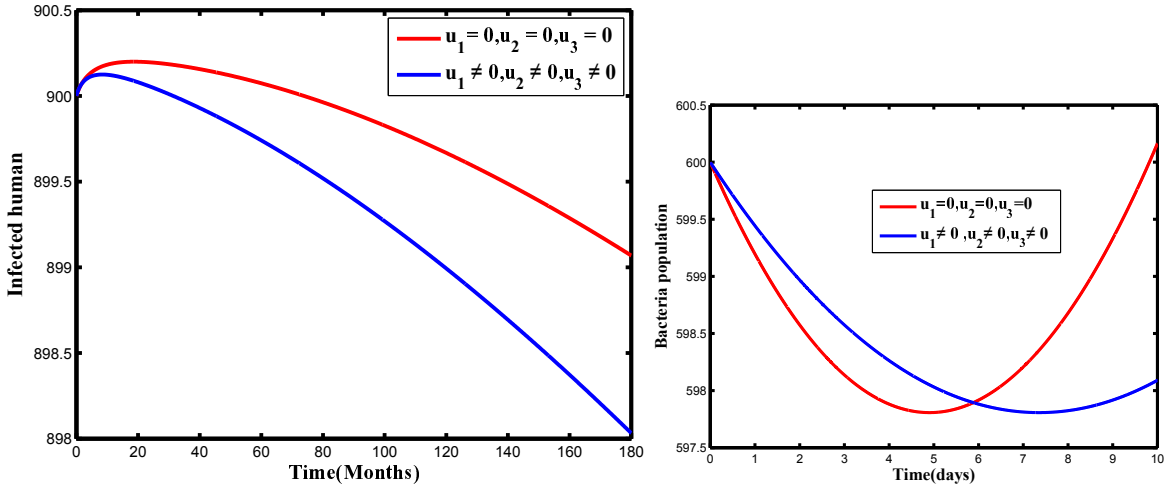

Fig. 13: Simulation of prevention,treatment and water sanitation

5.3 Cost-effectiveness Analysis

In this subsection, we have identified a strategy that is benefit compared to other strategies. To get this strategy, we used the method of incremental cost-effectiveness ratio (ICER), which is performed by dividing the difference of costs between two strategies to the difference of the total number of their infections averted. This approach was defined as follows:

$$ICER(A) = \frac{Cost of strategy A - Cost of Strategy B}{Total infections saved by Strategy A - Total infections saved by Strategy B}.$$

Applying one intervention only might to be effective to eliminate the disease from the community. Therefore, we analysed strategies that used more than one intervention method. In Table 3 we obtain the total number of infectious averted and total cost for the implemented strategies. To find the total cost for the applied strategies we used the cost function given by $\frac{1}{2}M_1u_1^2(t)$, $\frac{1}{2}M_2u_2^2(t)$and $\frac{1}{2}M_3u_3^2(t)$ over time. We used the parameter values in Table 2. and to apply *ICER* technique first we ordered the intervention strategies for pairwise comparison as in Table 3 from A to C with increasing order of effectiveness. First we in comparison the price effectiveness of approach A and B.

Table 3: Total amount of infection averted and total cost for all strategies.

Strategies	Description	Total infectious averted	Total cost ($)	ICER
A	Prevention and treatment	1,404.79	3564.75	2.534
B	Prevention and sanitation of water	4881.05	3813.248	0.0052
C	sanitation of water and treatment	5133.94	8118	16.96

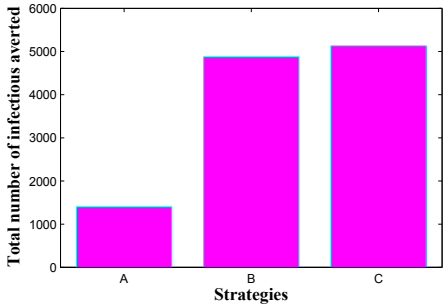

Fig. 14: Total infectious averted plots indicating the effect of control strategies A, B and C

$$ICER(A) = \frac{3564.75}{1404.79} = 2.534,,$$

$$ICER(B) = \frac{3813.248 - 3564.75}{48880.05 - 1404.79} = 0.0052,$$

$$ICER(C) = \frac{8118.98 - 3813.248}{5133.94 - 4880.05} = 16.96.$$

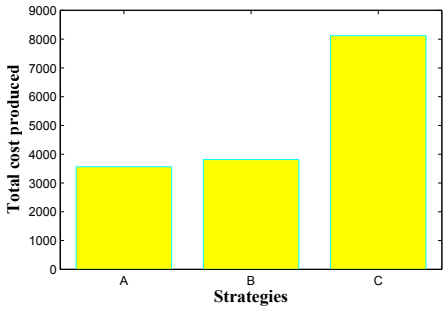

Fig. 15: Total infectious averted plots indicating the effect of control strategies A, B and C

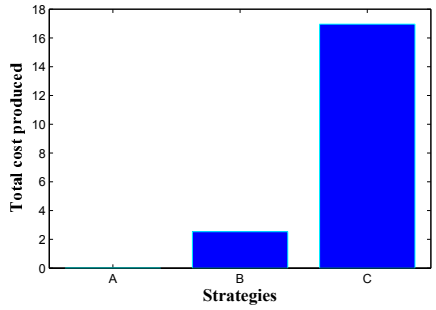

Fig. 16: Comparison of the ICER of each control

From ICER (A) and ICER (B) we can see that strategy B saves 0.0052 than strategy B. Therefore, we exclude strategy B, because it is a bit expensive and continue to compare strategy B and C. From ICER (B) and ICER (C) we can see that strategy A saves 0.0052 than strategy C. Therefore, we exclude strategy C, because it is a bit expensive. Therefore, we conclude that strategy B is the cheapest of all compared strategies, that meant it is the most cost-effective for cholera disease control interventions strategys.
The amount of people averted in strategies A, B and C in an increasing rank is given in Table 3. We can observe that, from the strategies A and B in Figure (16), the ICER (A) is less than ICER(B). This implies that strategy B is dominated by strategy A. It means that strategy B is more expensive than strategy A. Thus, we have deleted B from the strategies. For further explanation, we plotted a cost function graph, Figure (15) that shows applying only one intervention costs the least interims of price but we didn't consider this, due to the reason that a single intervention is not effective to eradicate the disease. Additionally, the figure indicates that, applying all the two intervention at once is the most expensive of all the applied intervention strategies. From the strategies A and B with their comparison in Table 3, we can observe that ICER (A) is less than ICER (B). This implies that strategy A is dominated by strategy B. It means that strategy B is more expensive than strategy A. Thus, we have deleted B from the comparison strategies. Then again re-calculate the ICER for the remaining comparison strategies A and C as given in Table 3

6 Results and Discussions

In this section, dynamics of cholera infection is described with analytical and numerical analysis. The fractional and optimal control effects are described. Moreover, the numerical simulation results obtained in Figure (3) shows that decreasing order of fractional derivative reduces the V. cholerae accumulation in the environment, the quarantine population size , the number of cholera infected individuals size decrease. Moreover, the numerical simulations results

obtained from Figure (5 -13) depicts the combined controls reduces the outbreak of infections in the community and ascend the cholera-free human population. Moreover, numerical simulation output indicates applying control strategy that includes control measures u_1 and u_3 from the beginning results in more effective techniques to manage further transmission of cholera disease. Moreover, applying prevention with treatment, and water sanitation is preferred among two and three controlling measures in the presence of cholera treatment. In Fig.4 the dynamics of individual size is simulated. The output shows that the numbers of susceptible individuals descend in the presence of cholera infection. The fractional derivative analysis results is supported by results achieved in [15]. In Figure (12), the impact of control strategies on the individuals is simulated along with associated coasts and applied control measures. The applied control reduces the number of infected individuals and V. cholerae concentration. Moreover, applying prevention controlling measures both on human and environment is effective from the starting to the end of the infection. The cost of applying all control is highly relative to others. However, the cost of including prevention and treatment in applying three control measures is less compared to other control measures. The optimal control analysis is supported with results obtained in [26,28].

7 Conclusion

In this study, we formulated mathematical model of cholera disease using Caputo fractional order to study the dynamics of cholera disease in the population taking into consideration memory effect. In Section 2, we described the model assumptions and formulated the deterministic model represented by systems of ordinary differential equations and the model extended to fractional order. In Section 3, model analysis was done by proving positively invariant region in which the solution to the fractional order model is bounded and non-negative, finding equilibrium points and basic reproduction number. Local and global stability analyses of both disease-free and endemic equilibrium points are presented. In Section 4, Extension of model into optimal control. In Section 5, numerical simulation was performed to investigate the effect of memory on cholera disease and we used MATLAB to perform numerical simulation. Applying numerical simulations, we investigated the impact of memory on the number of cholera-infected individuals,quarantine cholera individuals and bacteria population by using different values for the order of fractional derivative. Generally, our output shows that memory has great influence on disease dynamics and the result of the comparison between cholera-infected,quarantine cholera and bacteria population shows that decreasing order of fractional derivative is better to eliminate cholera disease from community. The dynamics of the cholera is complicated and needs further research both biologically and mathematically. Although the modern fractional order models developed in research study could produce better results in the comparison of existing classical models, we strongly believe that this research analysis can further be enhanced. However, we notice that the models with fractional derivatives are more complicated than the ones with classical derivatives. The authors declare that this manuscript is far from being complete because of the fact that the model does not fit to the cholera real data. It is a theoretical discussion with different assumptions on the parameters and initial state variables. Therefore, we recommend any interested researchers to apply the parameter estimation of cholera disease model for more novelty.

Acknowledgment(s)

The authors would like to express their gratitude to the anonymous referees for their helpful recommendations that helped to enhance the nice of this paper.

Funding

This research received no specific funding from public, private, or non-profit funding agencies.

References

[1] I. O. Fagbamila, Cholera outbreak in some communities in north-east nigeria, 2019: an unmatched case–control study. BMC Public Health, **23**(1), 446 (2023).

[2] H. M. Ali, F. L. Pereira and S. M. Gama, A new approach to the pontryagin maximum principle for nonlinear fractional optimal control problems, *Math. Meth. Appl. Sci.* **39**(13), 3640-3649 (2016).

[3] D. Biswas and S. Pal, Role of awareness to control transmission of HIV/AIDS epidemic with treatment and sensitivity analysis, *J. Stat. Manag. Syst.* **25**(3), 617-644 (2022

[4] S. F. Abimbade, S. Olaniyi, O. A. Ajala and M .O. Ibrahim, Optimal control analysis of a tuberculosis model with exogenous re-infection and incomplete treatment, *Opt. Contr. Appl. Meth.* **41**(6), 2349-2368 (2020).

[5] I. Ahmed, A. Yusuf, A. Ibrahim, P. Kumam and M. T. Ibrahim, A mathematical model of the ongoing coronavirus disease (COVID-19) pandemic: a case study in Turkey, *Sci. Tech. Asia*, **27**(4), 248-258 (2022).

[6] Y. Senderovich, I. Izhaki and M. Halpern, Fish as reservoirs and vectors of vibrio cholerae, *PloS one* **5**(1), e8607 (2010).

[7] M. S. Islam, M. H. Zaman, M. S. Islam, N. Ahmed and J. D. Clemens, Environmental reservoirs of vibrio cholerae, *Vaccine* **38**, A52-A62 (2020).

[8] D. Chac, C. N. Dunmire, J. Singh and A. A. Weil, Update on environmental and host factors impacting the risk of vibrio cholerae infection, *ACS Infect. Dis.* **7**(5), 1010-1019 (2021).

[9] G. T. Tilahun, W. A. Woldegerima and A. Wondifraw, Stochastic and deterministic mathematical model of cholera disease dynamics with direct transmission, *Adv. Differ. Equ.* **2020**, 670 (2020).

[10] K. Diethelm and N.J. Ford, Analysis of fractional differential equations,*J. Math. Anal. Appl.* **265**(2), 229-248 (2002).

[11] O. J. Peter, A. Qureshi,A. Yusuf, M. Al-Shomrani and A.A. Idowu, A new mathematical model of COVID-19 using real data from Pakistan, *Res. Phys.* **24**, 104098 (2021).

[12] A. A. Kilbas, H. M. Srivastava and J. J. Trujillo, Theory and Applications of Fractional Differential Equations (Vol. 204). Elsevier: Netherlands, (2006).

[13] S. Ucar, F. Evirgen, N. Ozdemir and Z. Hammouch, Mathematical analysis and simulation of a giving up smoking model within the scope of non-singular derivative, In Proceedings, Institute of Mathematics and Mechanics, National Academy of Sciences of Azerbaijan (Vol. 48) pp. 84-99, Baku, Azerbaijan, (2022).

[14] S. Uçar, Existence and uniqueness results for a smoking model with determination and education in the frame of non-singular derivatives *Discr. Cont. Dynam. System Ser. S* **14**(7), 2571-2589 (2021).

[15] U. Ullah, M. A. Khan, M. Farooq, Z. Hammouch and D. Baleanu, A fractional model for the dynamics of tuberculosis infection using Caputo-Fabrizio derivative, *Discr. Cont. Dynam. System Ser. S* **13**(3), (2020).

[16] F. Ozkose, R. Habbireeh and M. T. Senel, A novel fractional order model of SARS-CoV-2 and Cholera disease with real data, *J. Comput. Appl. Math.* **423**, 114969 (2023).

[17] I. Ahmed, E.F. D. Goufo, A. Yusuf, P. Kumam, P. Chaipanya and K. Nonlaopon, An epidemic prediction from analysis of a combined HIV-COVID-19 co-infection model via ABC-fractional operator, *Alexandria Eng. J.* **60**(3), 2979-2995 (2021).

[18] D. Baleanu, A. Jajarmi, H. Mohammadi and S. Rezapour, A new study on the mathematical modelling of human liver with Caputo-Fabrizio fractional derivative, *Chaos Solit. Fract.* **134**, 109705 (2020).

[19] J. Losada and J. J. Nieto, Properties of a new fractional derivative without singular kernel, *Progr. Fract. Differ. Appl.* **1**(2), 87-92 (2015).

[20] K. A. Eustace, S. Osman and M. Wainaina, Mathematical modelling and analysis of the dynamics of cholera, *Global J. Pure Appl. Math.* 14(9), 1259-1275 (2018).

[21] C. Ferreira, M. F. J. Doursout and J. S. Balingit, Syphilis, cholera, and yellow fever. In 2000 years of pandemics: Past, present, and future (pp. 79-97). Springer, (2023).

[22] A. A. Avwerosuo and A. M. Okedoye, Mathematical modelling of the dynamics and control of communicable diseases with emphasis on cholera epidemics, *Asian J. Appl. Sci. Techn. (AJAST)* **7**(4), 99-119 (2023).

[23] I. A. Baba, U. W. Humphries and F. A. Rihan, A well-posed fractional order cholera model with saturated incidence rate, *Entropy* **25**(2), 360 (2023).

[24] D. Baleanu, K. Diethelm, E. Scalas and J. J. Trujillo, Fractional calculus: models and numerical methods (Vol. 3), World Scientific (2012).

[25] M. Bergounioux and L. Bourdin, Pontryagin maximum principle for general caputo fractional optimal control problems with bolza cost and terminal constraints, *ESAIM: Contr. Optim. Calc. Var.C* **26**, 35 (2020).

[26] K. D. Brumfield, M. Usmani, K. M. Chen, M. Gangwar, A. S. Jutla, A. Huq, R. R. Colwell, Environmental parameters associated with incidence and transmission of pathogenic vibrio spp, *Environm. Micr.* **23**(12), 7314-7340 (2021).

[27] X. Cui, D. Xue and F. Pan, A fractional svir-b epidemic model for cholera with imperfect vaccination and saturated treatment, *Eur. Phys. J. Plus* **137**(12), 1361 (2022).

[28] N. V. Duc and T. P. Nguyen, A regularization method for caputo fractional derivatives in the banach space l[0, t], *Numer. Algorit.* **95**(2), 1033-1053 (2024).

[29] P. El Hayek et all. Cholera infection risks and cholera vaccine safety in pregnancy, *Infect. Dis. Obstetr. Gynec.* DOI:10.1155/2023/4563797, 1-8 (2023).

[30] A. Rautela et al., Chemotherapy for cancer treatment: An l1 optimal control approach, https://doi.org/10.21203/rs.3.rs-2746496/v1 (2023).

[31] D. Shackleton, F. A. Memon, G. Nichols, R. Phalke and A. S. Chen, Mechanisms of cholera transmission via environment in india and bangladesh: state of the science review, *Rev. Environ. Healt.* **1**, (2023).
[32] J. Wang, Mathematical models for cholera dynamicsa review, *Microorganisms* **10**(12) (2022). 2358.
[33] H. Yasmin, N. H. Aljahdaly, A. M. Saeed and R. Shah, Investigating families of soliton solutions for the complex structured coupled fractional biswas-arshed model in birefringent fibers using a novel analytical technique, *Fra. Fract.* **7**(7), 491 (2023).
[34] C. Kuehn and A. Neamt, Center manifolds for rough partial differential equations, *Electron. J. Probab.* 28:Paper No. **48**, 31 (2023).
[35] Z. Mukandavire, W. Garira and J. M. Tchuenche, Modelling effects of public health educational campaigns on HIV/AIDS transmission dynamics, *Appl. Math. Model.* **33**(4), 2084-2095 (2009).
[36] A. T. Layton and M. Sadria, Understanding the dynamics of SARS-CoV-2 variants of concern in Ontario, Canada: a modeling study, *Scient. Rep.* **12**, 2114 (2022).
[37] S. Duran, H. Durur, M. Yavuz and A. Yokus, Discussion of numerical and analytical techniques for the emerging fractional order murnaghan model in materials science, *Optic. Quant. Electr.* **55**, 571 (2023).
[38] G. Q. Sun, J. H. Xie, S. H. Huang, Z. Jin, M. T. Li and L. Liu, Transmission dynamics of cholera: mathematical modeling and control strategies, *Commun. Nonlin. Sci. Numer. Simul.* **45**, 235-244 (2017).
[39] A. Yokus, H. Durur, D. Kaya, H. Ahmad and T. A. Nofal, Numerical comparison of Caputo and conformable derivatives of time fractional Burgers-Fisher equation, *Res. Phys.* **25**, 104247 (2021).
[40] S. Ahmad, Q. I. U. Dong and R. U. Rahman, Dynamics of a fractional-order COVID-19 model under the nonsingular kernel of Caputo-Fabrizio operator, *Math. Model. Numer. Simul. Appl.* **2**(4), 228-243 (2022).
[41] A. O. Atede, A. Omame and S. C. A. Inyama, A fractional order vaccination model for COVID-19 incorporating environmental transmission: a case study using Nigerian data, *Bull. Biomath.* **1**(1), 78-110 (2023).
[42] I, Ahmed, A. Yusuf, M. A. Sani, F. Jarad, W. Kumam, W. and P. Thounthon, Analysis of a Caputo HIV and malaria co-infection epidemic model, *Thai J. Math.* **19**(3), 897-912 (2021).
[43] A. Hanif, A. I. K. Butt, S. Ahmad,R. U. Din and M. Inc, A new fuzzy fractional order model of transmission of Covid-19 with quarantine class, *Eur. Phys. J. Plus* **136**, 1179 (2021).
[44] H. Joshi, M. Yavuz and I. Stamova, Analysis of the disturbance effect in intracellular calcium dynamic on fibroblast cells with an exponential kernel law, *Bull. Biomath.* **1**(1), 24-39 (2023).
[45] S. Rashid, F. Jarad, H. Alsubaie, A.A. Aly and A. Alotaibi, A novel numerical dynamics of fractional derivatives involving singular and nonsingular kernels: designing a stochastic cholera epidemic model, *AIMS Math.* **8**(2), 3484-3522 (2023).
[46] A. Atangana and K. M. Owolabi, New numerical approach for fractional differential equations,*Math. Model. Nat. Phenom.* **13**(1), 3(2 018).